

Mitochondrial respiratory states and rates

COST Action CA15203 MitoEAGLE preprint Version: 2019-01-24 (52)

MitoEAGLE Task Group:

Gnaiger E, Aasander Frostner E, Abdul Karim N, Abumrad NA, Acuna-Castroviejo D, Adiele RC, Ahn B, Ali SS, Alton L, Alves MG, Amati F, Amoedo ND, Andreadou I, Aragón M, Aral C, Arandarčikaitė O, Armand AS, Arnould T, Avram VF, Bailey DM, Bajpeyi S, Bajzikova M, Bakker BM, Barlow J, Bastos Sant'Anna Silva AC, Batterson P, Battino M, Bazil J, Beard DA, Bednarczyk P, Bello F, Ben-Shachar D, Bergdahl A, Berge RK, Bergmeister L, Bernardi P, Berridge MV, Bettinazzi S, Bishop D, Blier PU, Blindheim DF, Boardman NT, Boetker HE, Borchard S, Boros M, Børshheim E, Borutaite V, Botella J, Bouillaud F, Bouitbir J, Boushel RC, Bovard J, Breton S, Brown DA, Brown GC, Brown RA, Brozinick JT, Buettner GR, Burtscher J, Calabria E, Calbet JA, Calzia E, Cannon DT, Cano Sanchez M, Canto AC, Cardoso LHD, Carvalho E, Casado Pinna M, Cassar S, Cassina AM, Castelo MP, Castro L, Cavalcanti-de-Albuquerque JP, Cervinkova Z, Chabi B, Chakrabarti L, Chakrabarti S, Chaurasia B, Chen Q, Chicco AJ, Chinopoulos C, Chowdhury SK, Cizmarova B, Clementi E, Coen PM, Cohen BH, Coker RH, Collin A, Crisóstomo L, Dahdah N, Dalgaard LT, Dambrova M, Danhelovska T, Darveau CA, Das AM, Dash RK, Davidova E, Davis MS, De Goede P, De Palma C, Dembinska-Kiec A, Detraux D, Devaux Y, Di Marcello M, Dias TR, Distefano G, Doermann N, Doerrier C, Dong L, Donnelly C, Drahota Z, Duarte FV, Dubouchaud H, Duchon MR, Dumas JF, Durham WJ, Dymkowska D, Dyrstad SE, Dyson A, Dzialowski EM, Eaton S, Ehinger J, Elmer E, Endlicher R, Engin AB, Escames G, Ezrova Z, Falk MJ, Fell DA, Ferdinandy P, Ferko M, Ferreira JCB, Ferreira R, Ferri A, Fessel JP, Filipovska A, Fisar Z, Fischer C, Fischer M, Fisher G, Fisher JJ, Ford E, Fornaro M, Galina A, Galkin A, Gallee L, Galli GL, Gan Z, Ganetzky R, Garcia-Rivas G, Garcia-Roves PM, Garcia-Souza LF, Garipi E, Garlid KD, Garrabou G, Garten A, Gastaldelli A, Gayen J, Genders AJ, Genova ML, Giovarelli M, Goncalo Teixeira da Silva R, Goncalves DF, Gonzalez-Armenta JL, Gonzalez-Freire M, Gonzalo H, Goodpaster BH, Gorr TA, Gourlay CW, Granata C, Grefte S, Guarch ME, Gueguen N, Gumeni S, Haas CB, Haavik J, Haendeler J, Haider M, Hamann A, Han J, Han WH, Hancock CR, Hand SC, Handl J, Hargreaves IP, Harper ME, Harrison DK, Hassan H, Hausenloy DJ, Heales SJR, Heiestad C, Hellgren KT, Hepple RT, Hernansanz-Agustin P, Hewakapuge S, Hickey AJ, Ho DH, Hoehn KL, Hoel F, Holland OJ, Holloway GP, Hoppel CL, Hoppel F, Houstek J, Huete-Ortega M, Hyrossova P, Iglesias-Gonzalez J, Irving BA, Isola R, Iyer S, Jackson CB, Jadiya P, Jana PF, Jang DH, Jang YC, Janowska J, Jansen K, Jansen-Dürr P, Jansone B, Jarmuszkiewicz W, Jaskiewicz A, Jedlicka J, Jespersen NR, Jha RK, Jurczak MJ, Jurk D, Kaambre T, Kaczor JJ, Kainulainen H, Kampa RP, Kandel SM, Kane DA, Kapferer W, Kappler L, Karabatsiakos A, Karkucinska-Wieckowska A, Kaur S, Keijer J, Keller MA, Keppner G, Khamoui AV, Kidere D, Kilbaugh T, Kim HK, Kim JKS, Klepinin A, Klepinina L, Klingenspor M, Klocker H, Komlodi T, Koopman WJH, Kopitar-Jerala N, Kowaltowski AJ, Kozlov AV, Krajcova A, Krako Jakovljevic N, Kristal BS, Krycer JR, Kuang J, Kucera O, Kuka J, Kwak HB, Kwast K, Laasmaa M, Labieniec-Watala M, Lai N, Land JM, Lane N, Laner V, Lanza IR, Larsen TS, Lavery GG, Lazou A, Lee HK, Leeuwenburgh C, Lehti M, Lemieux H, Lenaz G, Lerfall J, Li PA, Li Puma L, Liepins E, Lionett S, Liu J, López LC, Lucchinetti E, Ma T, Macedo MP, Maciej S, MacMillan-Crow LA, Majtnerova P, Makarova E, Makrecka-Kuka M, Malik AN, Markova M, Martin DS, Martins AD, Martins JD, Maseko TE, Maull F, Mazat JP, McKenna HT, Menze MA, Merz T, Meszaros AT, Methner A, Michalak S, Moellering DR, Moiso N, Molina AJA, Montaigne D, Moore AL, Moreau K, Moreno-Sánchez R, Moreira BP, Mracek T, Muccini AM, Muntane J, Muntean DM, Murray AJ, Musiol E,

49 Myhre Pedersen T, Nair KS, Nehlin JO, Nemeč M, Neuffer PD, Neuzil J, Neviere R, Newsom S,
 50 Nozickova K, O'Brien KA, O'Gorman D, Olgar Y, Oliveira B, Oliveira MF, Oliveira MT, Oliveira PF,
 51 Oliveira PJ, Orynbayeva Z, Osiewacz HD, Pak YK, Pallotta ML, Palmeira CM, Parajuli N, Passos JF,
 52 Passrigger M, Patel HH, Pavlova N, Pecina P, Pereira da Silva Grilo da Silva F, Perez Valencia JA,
 53 Perks KL, Pesta D, Petit PX, Pettersen IKN, Pichaud N, Pichler I, Piel S, Pietka TA, Pino MF, Pirkmajer
 54 S, Plangger M, Porter C, Porter RK, Procaccio V, Prochownik EV, Prola A, Pulinilkunnil T, Puskarich
 55 MA, Puurand M, Radenkovic F, Ramzan R, Rattan SIS, Reboredo P, Renner-Sattler K, Rial E, Robinson
 56 MM, Roden M, Rodriguez E, Rodriguez-Enriquez S, Rohlena J, Rolo AP, Ropelle ER, Røsland GV,
 57 Rossignol R, Rossiter HB, Rubelj I, Rybacka-Mossakowska J, Saada A, Safaei Z, Saharnaz S, Salin K,
 58 Salvadego D, Sandi C, Saner N, Sanz A, Sazanov LA, Scatena R, Schartner M, Scheibye-Knudsen M,
 59 Schilling JM, Schlattner U, Schönfeld P, Schots PC, Schulz R, Schwarzer C, Scott GR, Selman C,
 60 Shabalina IG, Sharma P, Sharma V, Shevchuk I, Shirazi R, Siewiera K, Silber AM, Silva AM, Sims
 61 CA, Singer D, Singh BK, Skolik R, Smenes BT, Smith J, Soares FAA, Sobotka O, Sokolova I, Sonkar
 62 VK, Sowton AP, Sparagna GC, Sparks LM, Spinazzi M, Stankova P, Starr J, Stary C, Stelfa G, Stepto
 63 NK, Stiban J, Stier A, Stocker R, Storder J, Sumbalova Z, Suomalainen A, Suravajhala P, Svalbe B,
 64 Swerdlow RH, Swiniuch D, Szabo I, Szewczyk A, Szibor M, Tanaka M, Tandler B, Tarnopolsky MA,
 65 Tausan D, Tavernarakis N, Tepp K, Thakkar H, Thapa M, Thyfault JP, Tomar D, Ton R, Torp MK,
 66 Towheed A, Tretter L, Trewin AJ, Trifunovic A, Trivigno C, Tronstad KJ, Trougakos IP, Truu L,
 67 Tuncay E, Turan B, Tyrrell DJ, Urban T, Valentine JM, Van Bergen NJ, Van Hove J, Varricchio F,
 68 Vella J, Vendelin M, Vercesi AE, Victor VM, Vieira Ligo Teixeira C, Vidimce J, Viel C, Vieyra A,
 69 Vilks K, Villena JA, Vincent V, Vinogradov AD, Viscomi C, Vitorino RMP, Vogt S, Volani C, Volska
 70 K, Votion DM, Vujacic-Mirski K, Wagner BA, Ward ML, Warnsmann V, Wasserman DH, Watala C,
 71 Wei YH, Whitfield J, Wickert A, Wieckowski MR, Wiesner RJ, Williams CM, Winwood-Smith H,
 72 Wohlgemuth SE, Wohlwend M, Wolff JN, Wrutniak-Cabello C, Wüst RCI, Yokota T, Zablocki K,
 73 Zanon A, Zaugg K, Zaugg M, Zdrzilova L, Zhang Y, Zhang YZ, Ziková A, Zischka H, Zorzano A,
 74 Zvejniece L

75
 76 Corresponding author: Gnaiger E

77 *Chair COST Action CA15203 MitoEAGLE* – <http://www.mitoeagle.org>

78 *Department of Visceral, Transplant and Thoracic Surgery, D. Swarovski Research Laboratory,*

79 *Medical University of Innsbruck, Innrain 66/4, A-6020 Innsbruck, Austria*

80 *Email: mitoeagle@i-med.ac.at; Tel: +43 512 566796, Fax: +43 512 566796 20*

81
 82 524 coauthors

83
 84 **Updates and discussion:**

85 http://www.mitoeagle.org/index.php/MitoEAGLE_preprint_States_and_rates



87	Table of contents
88	
89	Abstract
90	Executive summary
91	1. Introduction – Box 1: In brief: Mitochondria and Bioblasts
92	2. Coupling states and rates in mitochondrial preparations
93	2.1. <i>Cellular and mitochondrial respiration</i>
94	2.1.1. Aerobic and anaerobic catabolism and ATP turnover
95	2.1.2. Specification of biochemical dose
96	2.2. <i>Mitochondrial preparations</i>
97	2.3. <i>Electron transfer pathways</i>
98	2.4. <i>Respiratory coupling control</i>
99	2.4.1. Coupling
100	2.4.2. Phosphorylation, P _s , and P _s /O ₂ ratio
101	2.4.3. Uncoupling
102	2.5. <i>Coupling states and respiratory rates</i>
103	2.5.1. LEAK-state
104	2.5.2. OXPHOS-state
105	2.5.3. Electron transfer-state
106	2.5.4. ROX state and <i>Rox</i>
107	2.5.5. Quantitative relations
108	2.5.6. The steady-state
109	2.6. <i>Classical terminology for isolated mitochondria</i>
110	2.6.1. State 1
111	2.6.2. State 2
112	2.6.3. State 3
113	2.6.4. State 4
114	2.6.5. State 5
115	2.7. <i>Control and regulation</i>
116	3. What is a rate? – Box 2: Metabolic flows and fluxes: vectorial, vectorial, and scalar
117	4. Normalization of rate per sample
118	4.1. <i>Flow: per object</i>
119	4.1.1. Number concentration
120	4.1.2. Flow per object
121	4.2. <i>Size-specific flux: per sample size</i>
122	4.2.1. Sample concentration
123	4.2.2. Size-specific flux
124	4.3. <i>Marker-specific flux: per mitochondrial content</i>
125	4.3.1. Mitochondrial concentration and mitochondrial markers
126	4.3.2. mt-Marker-specific flux
127	5. Normalization of rate per system
128	5.1. <i>Flow: per chamber</i>
129	5.2. <i>Flux: per chamber volume</i>
130	5.2.1. System-specific flux
131	5.2.2. Advancement per volume
132	6. Conversion of units
133	7. Conclusions – Box 3: Recommendations for studies with mitochondrial preparations
134	Acknowledgements
135	Author contributions
136	Competing financial interests
137	References
138	Supplement
139	S1. Manuscript phases and versions - an open-access approach
140	S2. Joining COST Actions
141	

142 **Abstract** As the knowledge base and importance of mitochondrial physiology to human health expands,
 143 the necessity for harmonizing the terminology concerning mitochondrial respiratory states and rates has
 144 become increasingly apparent. The chemiosmotic theory establishes the mechanism of energy
 145 transformation and coupling in oxidative phosphorylation. The unifying concept of the protonmotive
 146 force provides the framework for developing a consistent theoretical foundation of mitochondrial
 147 physiology and bioenergetics. We follow guidelines of the International Union of Pure and Applied
 148 Chemistry (IUPAC) on terminology in physical chemistry, extended by considerations of open systems
 149 and thermodynamics of irreversible processes. The concept-driven constructive terminology
 150 incorporates the meaning of each quantity and aligns concepts and symbols with the nomenclature of
 151 classical bioenergetics. We endeavour to provide a balanced view of mitochondrial respiratory control
 152 and a critical discussion on reporting data of mitochondrial respiration in terms of metabolic flows and
 153 fluxes. Uniform standards for evaluation of respiratory states and rates will ultimately contribute to
 154 reproducibility between laboratories and thus support the development of databases of mitochondrial
 155 respiratory function in species, tissues, and cells. Clarity of concept and consistency of nomenclature
 156 facilitate effective transdisciplinary communication, education, and ultimately further discovery.

157
 158 *Keywords:* Mitochondrial respiratory control, coupling control, mitochondrial preparations,
 159 protonmotive force, uncoupling, oxidative phosphorylation: OXPHOS, efficiency, electron transfer: ET,
 160 electron transfer system: ETS, proton leak, ion leak and slip compensatory state: LEAK, residual oxygen
 161 consumption: ROX, State 2, State 3, State 4, normalization, flow, flux, oxygen: O₂
 162

163 **Executive summary**

164
 165 In view of the broad implications for health care, mitochondrial researchers face an increasing
 166 responsibility to disseminate their fundamental knowledge and novel discoveries to a wide range of
 167 stakeholders and scientists beyond the group of specialists. This requires implementation of a commonly
 168 accepted terminology within the discipline and standardization in the translational context. Authors,
 169 reviewers, journal editors, and lecturers are challenged to collaborate with the aim to harmonize the
 170 nomenclature in the growing field of mitochondrial physiology and bioenergetics, from evolutionary
 171 biology and comparative physiology to mitochondrial medicine. In the present communication we focus
 172 on the following concepts in mitochondrial physiology:

- 173 1. Aerobic respiration depends on the coupling of phosphorylation (ADP → ATP) to O₂ flux in
 174 catabolic reactions. Coupling in oxidative phosphorylation is mediated by the translocation of
 175 protons across the mitochondrial inner membrane (mtIM) through proton pumps generating
 176 or utilizing the protonmotive force that is maintained between the mitochondrial matrix and
 177 intermembrane compartment or outer mitochondrial space. Compartmental coupling depends
 178 on ion translocation across a semipermeable membrane, which is defined as vectorial
 179 metabolism and distinguishes oxidative phosphorylation from cytosolic fermentation as
 180 counterparts of cellular core energy metabolism (**Figure 1**). Cell respiration is thus
 181 distinguished from fermentation: (1) Electron acceptors are supplied by external respiration
 182 for the maintenance of redox balance, whereas fermentation is characterized by an internal
 183 electron acceptor produced in intermediary metabolism. In aerobic cell respiration, redox
 184 balance is maintained by O₂ as the electron acceptor. (2) Compartmental coupling in vectorial
 185 oxidative phosphorylation contrasts to exclusively scalar substrate-level phosphorylation in
 186 fermentation.
- 187 2. When measuring mitochondrial metabolism, the contribution of fermentation and other cytosolic
 188 interactions must be excluded from analysis by disrupting the barrier function of the plasma
 189 membrane. Selective removal or permeabilization of the plasma membrane yields
 190 mitochondrial preparations—including isolated mitochondria, tissue and cellular
 191 preparations—with structural and functional integrity. Subsequently, extra-mitochondrial
 192 concentrations of fuel substrates, ADP, ATP, inorganic phosphate, and cations including H⁺
 193 can be controlled to determine mitochondrial function under a set of conditions defined as
 194 coupling control states. We strive to incorporate an easily recognized and understood concept-
 195 driven terminology of bioenergetics with explicit terms and symbols that define the nature of
 196 respiratory states.

- 197 3. Mitochondrial coupling states are defined according to the control of respiratory oxygen flux by
 198 the protonmotive force. Capacities of oxidative phosphorylation and electron transfer are
 199 measured at kinetically saturating concentrations of fuel substrates, ADP and inorganic
 200 phosphate, and O₂, or at optimal uncoupler concentrations, respectively, in the absence of
 201 Complex IV inhibitors such as NO, CO, or H₂S. Respiratory capacity is a measure of the upper
 202 boundary of the rate of respiration; it depends on the substrate type undergoing oxidation, and
 203 provides reference values for the diagnosis of health and disease, and for evaluation of the
 204 effects of Evolutionary background, Age, Gender and sex, Lifestyle and Environment.
 205

206 Figure 1. Internal and external respiration

207 Mitochondrial respiration is the oxidation of fuel
 208 substrates (electron donors) and reduction of O₂
 209 catalysed by the electron transfer system, ETS:
 210 (mt) mitochondrial catabolic respiration; (ce)
 211 total cellular O₂ consumption; and (ext) external
 212 respiration. All chemical reactions, r , that
 213 consume O₂ in the cells of an organism,
 214 contribute to cell respiration, J_{O_2} . In addition to
 215 mitochondrial catabolic respiration, O₂ is
 216 consumed by:

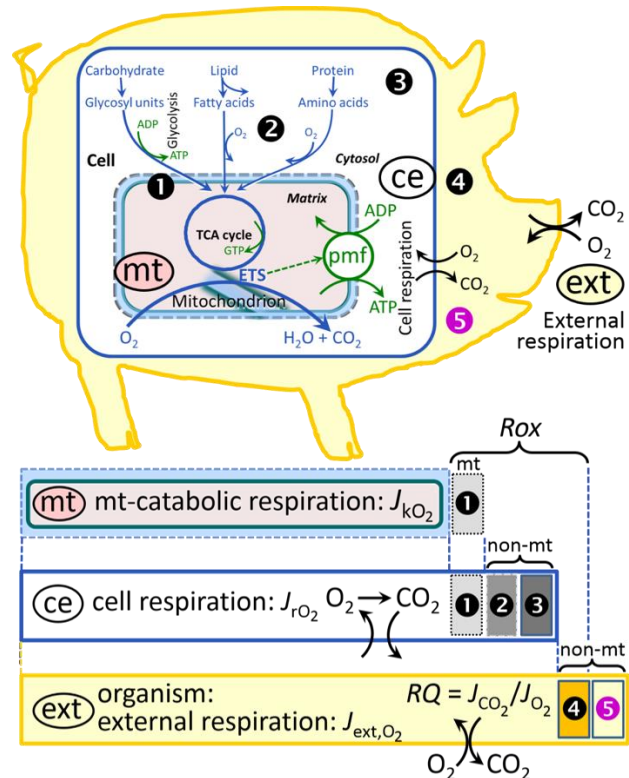
217 ❶ Mitochondrial residual oxygen consumption,
 218 R_{ox} . ❷ Non-mitochondrial O₂ consumption by
 219 catabolic reactions, particularly peroxisomal
 220 oxidases and microsomal cytochrome P450
 221 systems. ❸ Non-mitochondrial R_{ox} by reactions
 222 unrelated to catabolism. ❹ Extracellular R_{ox} . ❺
 223 Aerobic microbial respiration. Bars are not at a
 224 quantitative scale.

225 (mt) **Mitochondrial catabolic respiration**, $J_{\text{K}_{\text{O}_2}}$,
 226 is the O₂ consumption by the mitochondrial
 227 ETS excluding R_{ox} .

228 (ce) **Cell respiration**, J_{rO_2} , takes into account
 229 internal O₂-consuming reactions, r , including catabolic respiration and R_{ox} . Catabolic cell respiration
 230 is the O₂ consumption associated with catabolic pathways in the cell, including mitochondrial
 231 catabolism in addition to peroxisomal and microsomal oxidation reactions (❷).

232 (ext) **External respiration** balances internal respiration at steady-state, including extracellular R_{ox} (❹)
 233 and aerobic respiration by the microbiome (❺). O₂ is transported from the environment across the
 234 respiratory cascade, *i.e.*, circulation between tissues and diffusion across cell membranes, to the
 235 intracellular compartment. The respiratory quotient, RQ , is the molar CO₂/O₂ exchange ratio; when
 236 combined with the respiratory nitrogen quotient, N/O₂ (mol N given off per mol O₂ consumed), the
 237 RQ reflects the proportion of carbohydrate, lipid and protein utilized in cell respiration during
 238 aerobically balanced steady-states. Bicarbonate and CO₂ are transported in reverse to the
 239 extracellular milieu and the organismic environment. Hemoglobin provides the molecular paradigm
 240 for the combination of O₂ and CO₂ exchange, as do lungs and gills on the morphological level.
 241 Consult **Table 8** for a list of terms and symbols.
 242

- 243 4. Incomplete tightness of coupling, *i.e.*, some degree of uncoupling relative to the substrate-
 244 dependent coupling stoichiometry, is a characteristic of energy-transformations across
 245 membranes. Uncoupling is caused by a variety of physiological, pathological, toxicological,
 246 pharmacological and environmental conditions that exert an influence not only on the proton
 247 leak and cation cycling, but also on proton slip within the proton pumps and the structural
 248 integrity of the mitochondria. A more loosely coupled state is induced by stimulation of
 249 mitochondrial superoxide formation and the bypass of proton pumps. In addition, the use of
 250 protonophores represents an experimental uncoupling intervention to assess the transition
 251 from a well-coupled to a noncoupled state of mitochondrial respiration.



- 252 5. Respiratory oxygen consumption rates have to be carefully normalized to enable meta-analytic
 253 studies beyond the question of a particular experiment. Therefore, all raw data on rates and
 254 variables for normalization should be published in an open access data repository.
 255 Normalization of rates for: (1) the number of objects (cells, organisms); (2) the volume or
 256 mass of the experimental sample; and (3) the concentration of mitochondrial markers in the
 257 experimental chamber are sample-specific normalizations, which are distinguished from
 258 system-specific normalization for the volume of the chamber (the measuring system).
- 259 6. The consistent use of terms and symbols will facilitate transdisciplinary communication and
 260 support the further development of a collaborative database on bioenergetics and
 261 mitochondrial physiology. The present considerations are focused on studies with
 262 mitochondrial preparations. These will be extended in a series of reports on pathway control
 263 of mitochondrial respiration, respiratory states in intact cells, and harmonization of
 264 experimental procedures.
 265

266 **Box 1: In brief – Mitochondria and Bioblasts**

267 *‘For the physiologist, mitochondria afforded the first opportunity for an experimental*
 268 *approach to structure-function relationships, in particular those involved in active*
 269 *transport, vectorial metabolism, and metabolic control mechanisms on a subcellular level’*
 270 *(Ernster and Schatz 1981).*

271 Mitochondria are oxygen-consuming electrochemical generators that evolved from the endosymbiotic
 272 alphaproteobacteria which became integrated into a host cell related to Asgard Archaea (Margulis 1970;
 273 Lane 2005; Roger *et al.* 2017). They were described by Richard Altmann (1894) as ‘bioblasts’, which
 274 include not only the mitochondria as presently defined, but also symbiotic and free-living bacteria. The
 275 word ‘mitochondria’ (Greek mitos: thread; chondros: granule) was introduced by Carl Benda (1898).
 276 Mitochondrion is singular and mitochondria is plural. Abbreviation: mt, as generally used in mtDNA.

277 Contrary to current textbook dogma, which describes mitochondria as individual organelles,
 278 mitochondria form dynamic networks within eukaryotic cells. Mitochondrial movement is supported by
 279 microtubules and morphology can change in response to energy requirements of the cell via processes
 280 known as fusion and fission; these interactions allow mitochondria to communicate within a network
 281 (Chan 2006). Mitochondria can even traverse cell boundaries in a process known as horizontal
 282 mitochondrial transfer (Torralba *et al.* 2016). Another defining characteristic of mitochondria is the
 283 double membrane. The mitochondrial inner membrane (mtIM) forms dynamic tubular to disk-shaped
 284 cristae that separate the mitochondrial matrix, *i.e.*, the negatively charged internal mitochondrial
 285 compartment, from the intermembrane space; the latter being enclosed by the mitochondrial outer
 286 membrane (mtOM) and positively charged with respect to the matrix.

287 The mtIM contains the non-bilayer phospholipid cardiolipin, which is not present in any other
 288 eukaryotic cellular membrane. Cardiolipin has many regulatory functions (Oemer *et al.* 2018); in
 289 particular, it stabilizes and promotes the formation of respiratory supercomplexes (SC I_nIII_nIV_n), which
 290 are supramolecular assemblies based upon specific and dynamic interactions between individual
 291 respiratory complexes (Greggio *et al.* 2017; Lenaz *et al.* 2017). The mitochondrial membrane is plastic
 292 and exerts an influence on the functional properties of proteins incorporated in membranes
 293 (Waczulikova *et al.* 2007). Intracellular stress factors may cause shrinking or swelling of the
 294 mitochondrial matrix that can ultimately result in permeability transition (mtPT; Lemasters *et al.* 1998).

295 Mitochondria constitute the structural and functional elementary components of cell respiration.
 296 Mitochondrial respiration is the reduction of molecular oxygen by electron transfer coupled to
 297 electrochemical proton translocation across the mtIM. In the process of oxidative phosphorylation
 298 (OXPHOS), the catabolic reaction of oxygen consumption is electrochemically coupled to the
 299 transformation of energy in the form of adenosine triphosphate (ATP; Mitchell 1961, 2011).
 300 Mitochondria are the powerhouses of the cell that contain the machinery of the OXPHOS-pathways,
 301 including transmembrane respiratory complexes (proton pumps with FMN, Fe-S and cytochrome *b*, *c*,
 302 *aa*₃ redox systems); alternative dehydrogenases and oxidases; the coenzyme ubiquinone (Q); F-ATPase
 303 or ATP synthase; the enzymes of the tricarboxylic acid cycle (TCA), fatty acid and amino acid oxidation;
 304 transporters of ions, metabolites and co-factors; iron/sulphur cluster synthesis; and mitochondrial
 305 kinases related to catabolic pathways. The mitochondrial proteome comprises over 1,200 proteins
 306 (Calvo *et al.* 2015; 2017), mostly encoded by nuclear DNA (nDNA), with a variety of functions, many
 307 of which are relatively well known, *e.g.*, proteins regulating mitochondrial biogenesis or apoptosis,

308 while others are still under investigation, or need to be identified, *e.g.*, mtPT pore, alanine transporter.
309 The mammalian mitochondrial proteome can be used to discover and characterize the genetic basis of
310 mitochondrial diseases (Williams *et al.* 2016; Palmfeldt and Bross 2017).

311 Numerous cellular processes are orchestrated by a constant crosstalk between mitochondria and
312 other cellular components. For example, the crosstalk between mitochondria and the endoplasmic
313 reticulum is involved in the regulation of calcium homeostasis, cell division, autophagy, differentiation,
314 and anti-viral signaling (Murley and Nunnari 2016). Mitochondria contribute to the formation of
315 peroxisomes, which are hybrids of mitochondrial and ER-derived precursors (Sugiura *et al.* 2017).
316 Cellular mitochondrial homeostasis (mitostasis) is maintained through regulation at transcriptional,
317 post-translational and epigenetic levels, resulting in dynamic regulation of mitochondrial turnover by
318 biogenesis of new mitochondria and removal of damaged mitochondria by fusion, fission and mitophagy
319 (Singh *et al.* 2018). Cell signalling modules contribute to homeostatic regulation throughout the cell
320 cycle or even cell death by activating proteostatic modules, *e.g.*, the ubiquitin-proteasome and
321 autophagy-lysosome/vacuole pathways; specific proteases like LON, and genome stability modules in
322 response to varying energy demands and stress cues (Quiros *et al.* 2016). Several post-translational
323 modifications, including acetylation and nitrosylation, are also capable of influencing the bioenergetic
324 response, with clinically significant implications for health and disease (Carrico *et al.* 2018).

325 Mitochondria of higher eukaryotes typically maintain several copies of their own circular genome
326 known as mitochondrial DNA (mtDNA; hundred to thousands per cell; Cummins 1998), which is
327 maternally inherited in many species. However, biparental mitochondrial inheritance is documented in
328 some exceptional cases in humans (Luo *et al.* 2018), is widespread in birds, fish, reptiles and invertebrate
329 groups, and is even the norm in some bivalve taxonomic groups (Breton *et al.* 2007; White *et al.* 2008).
330 The mitochondrial genome of the angiosperm *Amborella* contains a record of six mitochondrial genome
331 equivalents acquired by horizontal transfer of entire genomes, two from angiosperms, three from algae
332 and one from mosses (Rice *et al.* 2016). In unicellular organisms, *i.e.*, protists, the structural organization
333 of mitochondrial genomes is highly variable and includes circular and linear DNA (Zikova *et al.* 2016).
334 While some of the free-living flagellates exhibit the largest known gene coding capacity, *e.g.*, jakobid
335 *Andalucia godoyi* mitochondrial DNA codes for 106 genes (Burger *et al.* 2013), some protist groups,
336 *e.g.*, alveolates, possess mitochondrial genomes with only three protein-coding genes and two rRNAs
337 (Feagin *et al.* 2012). The complete loss of mitochondrial genome is observed in the highly reduced
338 mitochondria of *Cryptosporidium* species (Liu *et al.* 2016). Reaching the final extreme, the microbial
339 eukaryote, oxymonad *Monocercomonoides*, has no mitochondrion whatsoever and lacks all typical
340 nuclear-encoded mitochondrial proteins, showing that while in 99% of organisms mitochondria play a
341 vital role, this organelle is not indispensable (Karnkowska *et al.* 2016).

342 In vertebrates, but not all invertebrates, mtDNA is compact (16.5 kB in humans) and encodes 13
343 protein subunits of the transmembrane respiratory Complexes CI, CIII, CIV and ATP synthase (F-
344 ATPase), 22 tRNAs, and two ribosomal RNAs. Additional gene content has been suggested to include
345 microRNAs, piRNA, smithRNAs, repeat associated RNA, long noncoding RNAs, and even additional
346 proteins or peptides (Rackham *et al.* 2011; Duarte *et al.* 2014; Lee *et al.* 2015; Cobb *et al.* 2016). The
347 mitochondrial genome requires nuclear-encoded mitochondrially targeted proteins, *e.g.*, TFAM, for its
348 maintenance and expression (Rackham *et al.* 2012). The nuclear and the mitochondrial genomes encode
349 peptides of the membrane spanning redox pumps (CI, CIII and CIV) and F-ATPase, leading to strong
350 constraints in the coevolution of both genomes (Blier *et al.* 2001).

351 Given the multiple roles of mitochondria, it is perhaps not surprising that mitochondrial
352 dysfunction is associated with a wide variety of genetic and degenerative diseases. Robust mitochondrial
353 function is supported by physical exercise and caloric balance, and is central for sustained metabolic
354 health throughout life. Therefore, a more consistent set of definitions for mitochondrial physiology will
355 increase our understanding of the etiology of disease and improve the diagnostic repertoire of
356 mitochondrial medicine with a focus on protective medicine, lifestyle and healthy aging.

358
359

360 1. Introduction

361
362
363

Mitochondria are the powerhouses of the cell with numerous physiological, molecular, and genetic functions (**Box 1**). Every study of mitochondrial health and disease faces **Evolution, Age,**

364 **Gender and sex, Lifestyle, and Environment (MitoEAGLE)** as essential background conditions intrinsic
 365 to the individual person or cohort, species, tissue and to some extent even cell line. As a large and
 366 coordinated group of laboratories and researchers, the mission of the global MitoEAGLE Network is to
 367 generate the necessary scale, type, and quality of consistent data sets and conditions to address this
 368 intrinsic complexity. Harmonization of experimental protocols and implementation of a quality control
 369 and data management system are required to interrelate results gathered across a spectrum of studies
 370 and to generate a rigorously monitored database focused on mitochondrial respiratory function. In this
 371 way, researchers from a variety of disciplines can compare their findings using clearly defined and
 372 accepted international standards.

373 With an emphasis on quality of research, published data can be useful far beyond the specific
 374 question of a particular experiment. For example, collaborative data sets support the development of
 375 open-access databases such as those for National Institutes of Health sponsored research in genetics,
 376 proteomics, and metabolomics. Indeed, enabling meta-analysis is the most economic way of providing
 377 robust answers to biological questions (Cooper *et al.* 2009). However, the reproducibility of quantitative
 378 results and databases depend on accurate measurements under strictly-defined conditions. Likewise,
 379 meaningful interpretation and comparability of experimental outcomes requires standardisation of
 380 protocols between research groups at different institutes. In addition to quality control, a conceptual
 381 framework is also required to standardise and harmonise terminology and methodology. Vague or
 382 ambiguous jargon can lead to confusion and may convert valuable signals to wasteful noise. For this
 383 reason, measured values must be expressed in standard units for each parameter used to define
 384 mitochondrial respiratory function. A consensus on fundamental nomenclature and conceptual
 385 coherence, however, are missing in the expanding field of mitochondrial physiology. To fill this gap,
 386 the present communication provides an in-depth review on harmonization of nomenclature and
 387 definition of technical terms, which are essential to improve the awareness of the intricate meaning of
 388 current and past scientific vocabulary. This is important for documentation and integration into
 389 databases in general, and quantitative modelling in particular (Beard 2005).

390 In this review, we focus on coupling states and fluxes through metabolic pathways of aerobic
 391 energy transformation in mitochondrial preparations as a first step in the attempt to generate a
 392 conceptually-oriented nomenclature in bioenergetics and mitochondrial physiology. Respiratory control
 393 by fuel substrates and specific inhibitors of respiratory enzymes, coupling states of intact cells, and
 394 respiratory flux control ratios will be reviewed in subsequent communications, prepared in the frame of
 395 the EU COST Action MitoEAGLE open to global bottom-up input.

396
397

398 **2. Coupling states and rates in mitochondrial preparations**

399 *‘Every professional group develops its own technical jargon for talking about matters of critical*
 400 *concern ... People who know a word can share that idea with other members of their group, and*
 401 *a shared vocabulary is part of the glue that holds people together and allows them to create a*
 402 *shared culture’* (Miller 1991).

403

404 *2.1. Cellular and mitochondrial respiration*

405

406 **2.1.1. Aerobic and anaerobic catabolism and ATP turnover:** In respiration, electron transfer
 407 is coupled to the phosphorylation of ADP to ATP, with energy transformation mediated by the
 408 protonmotive force, pmf (**Figure 2**). Anabolic reactions are coupled to catabolism, both by ATP as the
 409 intermediary energy currency and by small organic precursor molecules as building blocks for
 410 biosynthesis. Glycolysis involves substrate-level phosphorylation of ADP to ATP in fermentation
 411 without utilization of O₂, studied mainly in intact cells and organisms. Many cellular fuel substrates are
 412 catabolized to acetyl-CoA or to glutamate, and further electron transfer reduces nicotinamide adenine
 413 dinucleotide to NADH or flavin adenine dinucleotide to FADH₂. Subsequent mitochondrial electron
 414 transfer to O₂ is coupled to proton translocation for the control of the protonmotive force and
 415 phosphorylation of ADP (**Figure 2B and 2C**). In contrast, extra-mitochondrial oxidation of fatty acids
 416 and amino acids proceeds partially in peroxisomes without coupling to ATP production: acyl-CoA
 417 oxidase catalyzes the oxidation of FADH₂ with electron transfer to O₂; amino acid oxidases oxidize
 418 flavin mononucleotide FMNH₂ or FADH₂ (**Figure 2A**).

419

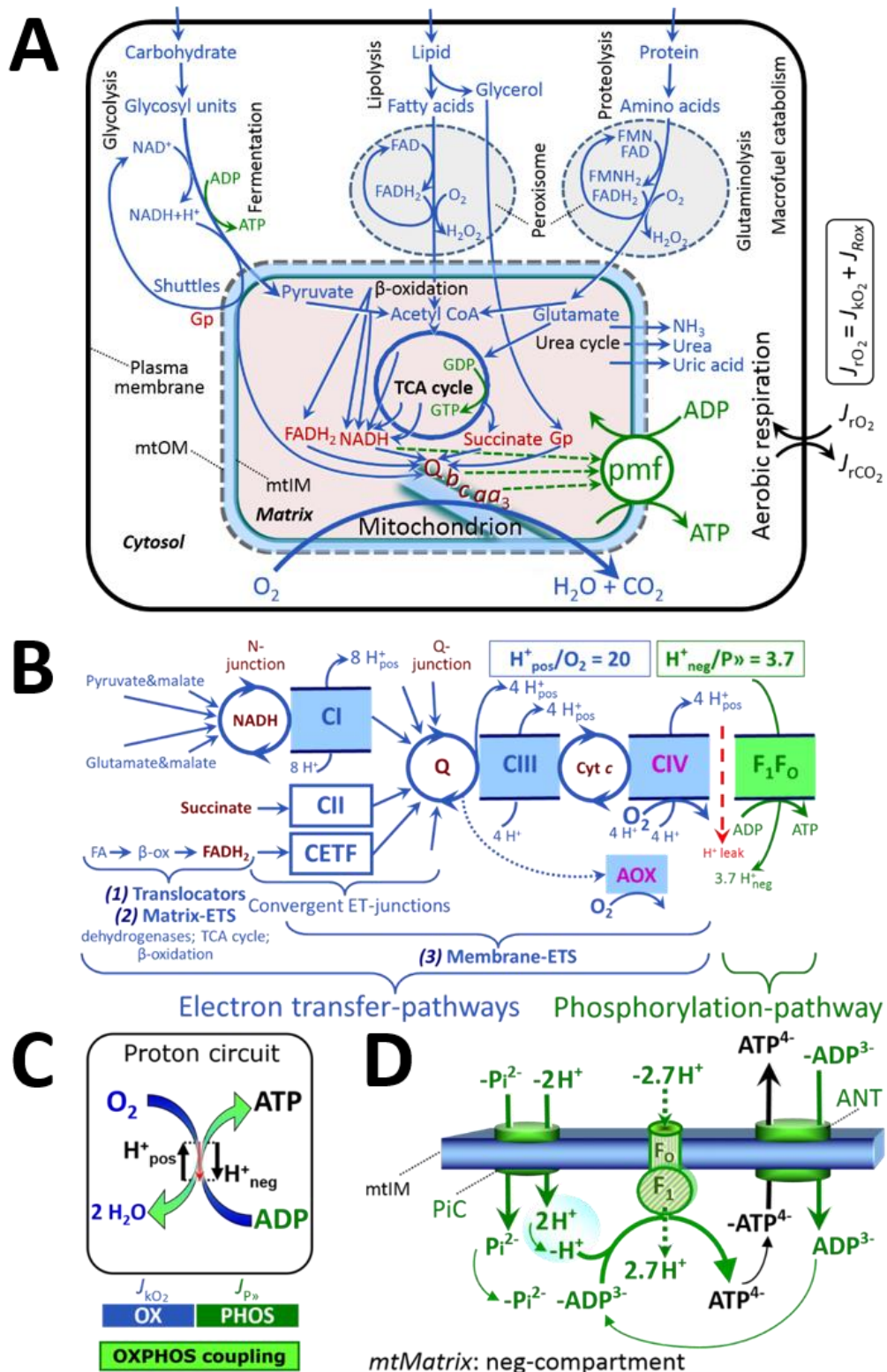


Figure 2. Cell respiration and oxidative phosphorylation (OXPHOS)

Mitochondrial respiration is the oxidation of fuel substrates (electron donors) with electron transfer to O_2 as the electron acceptor. For explanation of symbols see also **Figure 1**.

(A) Respiration of intact cells: Extra-mitochondrial catabolism of macrofuels and uptake of small molecules by the cell provide the mitochondrial fuel substrates. Dashed arrows indicate the connection between the redox proton pumps (respiratory Complexes CI, CIII and CIV) and the transmembrane protonmotive force, pmf. Coenzyme Q (Q) and the cytochromes *b*, *c*, and *aa₃* are redox systems of the mitochondrial inner membrane, mtIM. Glycerol-3-phosphate, Gp.

420
421
422
423
424
425
426
427
428
429

430 (B) Respiration in mitochondrial preparations: The mitochondrial electron transfer system
 431 (ETS) is (1) fuelled by diffusion and transport of substrates across the mtOM and mtIM,
 432 and in addition consists of the (2) matrix-ETS, and (3) membrane-ETS. Electron transfer
 433 converges at the N-junction, and from CI, CII and electron transferring flavoprotein
 434 complex (CETF) at the Q-junction. Unlabeled arrows converging at the Q-junction indicate
 435 additional ETS-sections with electron entry into Q through glycerophosphate
 436 dehydrogenase, dihydroorotate dehydrogenase, proline dehydrogenase, choline
 437 dehydrogenase, and sulfide-ubiquinone oxidoreductase. The dotted arrow indicates the
 438 branched pathway of oxygen consumption by alternative quinol oxidase (AOX). ET-
 439 pathways are coupled to the phosphorylation-pathway. The H^+_{pos}/O_2 ratio is the outward
 440 proton flux from the matrix space to the positively (pos) charged vesicular compartment,
 441 divided by catabolic O_2 flux in the NADH-pathway. The H^+_{neg}/P_{\gg} ratio is the inward proton
 442 flux from the inter-membrane space to the negatively (neg) charged matrix space, divided
 443 by the flux of phosphorylation of ADP to ATP. These stoichiometries are not fixed because
 444 of ion leaks and proton slip. Modified from Lemieux *et al.* (2017) and Rich (2013).
 445 (C) OXPHOS coupling: O_2 flux through the catabolic ET-pathway, J_{kO_2} , is coupled
 446 by the H^+ circuit to flux through the phosphorylation-pathway of ADP to ATP, $J_{P_{\gg}}$.
 447 (D) Phosphorylation-pathway catalyzed by the proton pump F_1F_0 -ATPase (F-ATPase,
 448 ATP synthase), adenine nucleotide translocase (ANT), and inorganic phosphate carrier
 449 (PiC). The H^+_{neg}/P_{\gg} stoichiometry is the sum of the coupling stoichiometry in the F-ATPase
 450 reaction ($-2.7 H^+_{\text{pos}}$ from the positive intermembrane space, $2.7 H^+_{\text{neg}}$ to the matrix, *i.e.*, the
 451 negative compartment) and the proton balance in the translocation of ADP^{3-} , ATP^{4-} and P_i^{2-}
 452 (negative for substrates). Modified from Gnaiger (2014).
 453

454 The plasma membrane separates the intracellular compartment including the cytosol, nucleus, and
 455 organelles from the extracellular environment. The plasma membrane consists of a lipid bilayer with
 456 embedded proteins and attached organic molecules that collectively control the selective permeability
 457 of ions, organic molecules, and particles across the cell boundary. The intact plasma membrane prevents
 458 the passage of many water-soluble mitochondrial substrates and inorganic ions—such as succinate,
 459 adenosine diphosphate (ADP) and inorganic phosphate (P_i) that must be precisely controlled at
 460 kinetically-saturating concentrations for the analysis of mitochondrial respiratory capacities.
 461 Respiratory capacities delineate, comparable to channel capacity in information theory (Schneider
 462 2006), the upper boundary of the rate of O_2 consumption measured in defined respiratory states. Despite
 463 the activity of solute carriers, *e.g.*, the sodium-dependent dicarboxylate transporter SLC13A3 and the
 464 sodium-dependent phosphate transporter SLC20A2, which transport specific metabolites across the
 465 plasma membrane of various cell types, the intact plasma membrane limits the scope of investigations
 466 into mitochondrial respiratory function in intact cells.

467 **2.1.2. Specification of biochemical dose:** Substrates, uncouplers, inhibitors, and other chemical
 468 reagents are titrated to analyse cellular and mitochondrial function. Nominal concentrations of these
 469 substances are usually reported as initial amount of substance concentration [$\text{mol}\cdot\text{L}^{-1}$] in the incubation
 470 medium. When aiming at the measurement of kinetically saturated processes—such as OXPHOS-
 471 capacities—the concentrations for substrates can be chosen according to the apparent equilibrium
 472 constant, K_m' . In the case of hyperbolic kinetics, only 80% of maximum respiratory capacity is obtained
 473 at a substrate concentration of four times the K_m' , whereas substrate concentrations of 5, 9, 19 and 49
 474 times the K_m' are theoretically required for reaching 83%, 90%, 95% or 98% of the maximal rate
 475 (Gnaiger 2001). Other reagents are chosen to inhibit or alter a particular process. The amount of these
 476 chemicals in an experimental incubation is selected to maximize effect, avoiding unacceptable off-target
 477 consequences that would adversely affect the data being sought. Specifying the amount of substance in
 478 an incubation as nominal concentration in the aqueous incubation medium can be ambiguous (Doskey
 479 *et al.* 2015), particularly for cations (TPP⁺; fluorescent dyes such as safranin, TMRM; Chowdhury *et al.*
 480 2015) and lipophilic substances (oligomycin, uncouplers, permeabilization agents; Doerrier *et al.* 2018),
 481 which accumulate in the mitochondrial matrix or in biological membranes, respectively. Generally,
 482 dose/exposure can be specified per unit of biological sample, *i.e.*, (nominal moles of
 483 xenobiotic)/(number of cells) [$\text{mol}\cdot\text{cell}^{-1}$] or, as appropriate, per mass of biological sample [$\text{mol}\cdot\text{kg}^{-1}$].
 484 This approach to specification of dose/exposure provides a scalable parameter that can be used to design

485 experiments, help interpret a wide variety of experimental results, and provide absolute information that
486 allows researchers worldwide to make the most use of published data (Doskey *et al.* 2015).

487

488 2.2. Mitochondrial preparations

489

490 Mitochondrial preparations are defined as either isolated mitochondria or tissue and cellular
491 preparations in which the barrier function of the plasma membrane is disrupted. Since this entails the
492 loss of cell viability, mitochondrial preparations are not studied *in vivo*. In contrast to isolated
493 mitochondria and tissue homogenate preparations, mitochondria in permeabilized tissues and cells are
494 *in situ* relative to the plasma membrane. When studying mitochondrial preparations, substrate-
495 uncoupler-inhibitor-titration (SUIT) protocols are used to establish respiratory coupling control states
496 (CCS) and pathway control states (PCS) that provide reference values for various output variables
497 (Table 1). Physiological conditions *in vivo* deviate from these experimentally obtained states; this is
498 because kinetically-saturating concentrations, *e.g.*, of ADP, oxygen (O₂; dioxygen) or fuel substrates,
499 may not apply to physiological intracellular conditions. Further information is obtained in studies of
500 kinetic responses to variations in fuel substrate concentrations, [ADP], or [O₂] in the range between
501 kinetically-saturating concentrations and anoxia (Gnaiger 2001).

502 The cholesterol content of the plasma membrane is high compared to mitochondrial membranes
503 (Korn 1969). Therefore, mild detergents—such as digitonin and saponin—can be applied to selectively
504 permeabilize the plasma membrane via interaction with cholesterol; this allows free exchange of organic
505 molecules and inorganic ions between the cytosol and the immediate cell environment, while
506 maintaining the integrity and localization of organelles, cytoskeleton, and the nucleus. Application of
507 permeabilization agents (mild detergents or toxins) leads to washout of cytosolic marker enzymes—
508 such as lactate dehydrogenase—and results in the complete loss of cell viability (tested by nuclear
509 staining using plasma membrane-impermeable dyes), while mitochondrial function remains intact
510 (tested by cytochrome *c* stimulation of respiration). Digitonin concentrations have to be optimized
511 according to cell type, particularly since mitochondria from cancer cells contain significantly higher
512 contents of cholesterol in both membranes (Baggetto and Testa-Perussini, 1990). For example, a dose
513 of digitonin of 8 fmol·cell⁻¹ (10 pg·cell⁻¹; 10 μg·10⁻⁶ cells) is optimal for permeabilization of endothelial
514 cells, and the concentration in the incubation medium has to be adjusted according to the cell density
515 (Doerrier *et al.* 2018). Respiration of isolated mitochondria remains unaltered after the addition of low
516 concentrations of digitonin or saponin. In addition to mechanical cell disruption during homogenization
517 of tissue, permeabilization agents may be applied to ensure permeabilization of all cells in tissue
518 homogenates.

519 Suspensions of cells permeabilized in the respiration chamber and crude tissue homogenates
520 contain all components of the cell at highly dilute concentrations. All mitochondria are retained in
521 chemically-permeabilized mitochondrial preparations and crude tissue homogenates. In the preparation
522 of isolated mitochondria, however, the mitochondria are separated from other cell fractions and purified
523 by differential centrifugation, entailing the loss of mitochondria at typical recoveries ranging from 30%
524 to 80% of total mitochondrial content (Lai *et al.* 2018). Using Percoll or sucrose density gradients to
525 maximize the purity of isolated mitochondria may compromise the mitochondrial yield or structural and
526 functional integrity. Therefore, mitochondrial isolation protocols need to be optimized according to each
527 study. The term, *mitochondrial preparation*, neither includes intact cells, nor submitochondrial particles
528 and further fractionated mitochondrial components.

529

530 2.3. Electron transfer pathways

531

532 Mitochondrial electron transfer (ET) pathways are fuelled by diffusion and transport of substrates
533 across the mtOM and mtIM. In addition, the mitochondrial electron transfer system (ETS) consists of
534 the matrix-ETS and membrane-ETS (Figure 2B). Upstream sections of ET-pathways converge at the
535 NADH-junction (N-junction). NADH is mainly generated in the tricarboxylic acid (TCA) cycle and is
536 oxidized by Complex I (CI), with further electron entry into the coenzyme Q-junction (Q-junction).
537 Similarly, succinate is formed in the TCA cycle and oxidized by CII to fumarate. CII is part of both the
538 TCA cycle and the ETS, and reduces FAD to FADH₂ with further reduction of ubiquinone to ubiquinol
539 downstream of the TCA cycle in the Q-junction. Thus FADH₂ is not a substrate but is the product of
540 CII, in contrast to erroneous metabolic maps shown in many publications. β-oxidation of fatty acids

541 (FA) supplies reducing equivalents via (1) FADH₂ as the substrate of electron transferring flavoprotein
 542 complex (CETF); (2) acetyl-CoA generated by chain shortening; and (3) NADH generated via 3-
 543 hydroxyacyl-CoA dehydrogenases. The ATP yield depends on whether acetyl-CoA enters the TCA
 544 cycle, or is for example used in ketogenesis.

545 Selected mitochondrial catabolic pathways, *k*, of electron transfer from the oxidation of fuel
 546 substrates to the reduction of O₂ are activated by addition of fuel substrates to the mitochondrial
 547 respiration medium after depletion of endogenous substrates (**Figure 2B**). Substrate combinations and
 548 specific inhibitors of ET-pathway enzymes are used to obtain defined pathway control states in
 549 mitochondrial preparations (Gnaiger 2014).

550

551 2.4. Respiratory coupling control

552

553 **2.4.1. Coupling:** In mitochondrial electron transfer, vectorial transmembrane proton flux is
 554 coupled through the redox proton pumps CI, CIII and CIV to the catabolic flux of scalar reactions,
 555 collectively measured as O₂ flux, J_{kO_2} (**Figure 2**). Thus mitochondria are elementary components of
 556 energy transformation. Energy is a conserved quantity and cannot be lost or produced in any internal
 557 process (First Law of Thermodynamics). Open and closed systems can gain or lose energy only by
 558 external fluxes—by exchange with the environment. Therefore, energy can neither be produced by
 559 mitochondria, nor is there any internal process without energy conservation. Exergy or Gibbs energy
 560 (‘free energy’) is the part of energy that can potentially be transformed into work under conditions of
 561 constant temperature and pressure. *Coupling* is the interaction of an exergonic process (spontaneous,
 562 negative exergy change) with an endergonic process (positive exergy change) in energy transformations
 563 which conserve part of the exergy that would be irreversibly lost or dissipated in an uncoupled process.

564 Pathway control states (PCS) and coupling control states (CCS) are complementary, since
 565 mitochondrial preparations depend on (1) an exogenous supply of pathway-specific fuel substrates and
 566 oxygen, and (2) exogenous control of phosphorylation (**Figure 2**).

567 **2.4.2. Phosphorylation, P_», and P_»/O₂ ratio:** Phosphorylation in the context of OXPHOS is
 568 defined as phosphorylation of ADP by P_i to form ATP. On the other hand, the term phosphorylation is
 569 used generally in many contexts, *e.g.*, protein phosphorylation. This justifies consideration of a symbol
 570 more discriminating and specific than P as used in the P/O ratio (phosphate to atomic oxygen ratio),
 571 where P indicates phosphorylation of ADP to ATP or GDP to GTP (**Figure 2**). We propose the symbol
 572 P_» for the endergonic (uphill) direction of phosphorylation ADP→ATP, and likewise the symbol P_« for
 573 the corresponding exergonic (downhill) hydrolysis ATP→ADP. P_» refers mainly to electrontransfer
 574 phosphorylation but may also involve substrate-level phosphorylation as part of the TCA cycle
 575 (succinyl-CoA ligase, phosphoglycerate kinase) and phosphorylation of ADP catalyzed by pyruvate
 576 kinase, and of GDP phosphorylated by phosphoenolpyruvate carboxykinase. Transphosphorylation is
 577 performed by adenylate kinase, creatine kinase (mtCK), hexokinase and nucleoside diphosphate kinase.
 578 In isolated mammalian mitochondria, ATP production catalyzed by adenylate kinase (2 ADP ↔ ATP +
 579 AMP) proceeds without fuel substrates in the presence of ADP (Kömldi and Tretter 2017). Kinase
 580 cycles are involved in intracellular energy transfer and signal transduction for regulation of energy flux.

581 The P_»/O₂ ratio (P_»/4 e⁻) is two times the ‘P/O’ ratio (P_»/2 e⁻). P_»/O₂ is a generalized symbol, not
 582 specific for reporting P_i consumption (P_i/O₂ flux ratio), ADP depletion (ADP/O₂ flux ratio), or ATP
 583 production (ATP/O₂ flux ratio). The mechanistic P_»/O₂ ratio—or P_»/O₂ stoichiometry—is calculated
 584 from the proton-to-O₂ and proton-to-phosphorylation coupling stoichiometries (**Figure 2B**):

$$586 \quad P_{\gg}/O_2 = \frac{H_{pos}^+/O_2}{H_{neg}^+/P_{\gg}} \quad (1)$$

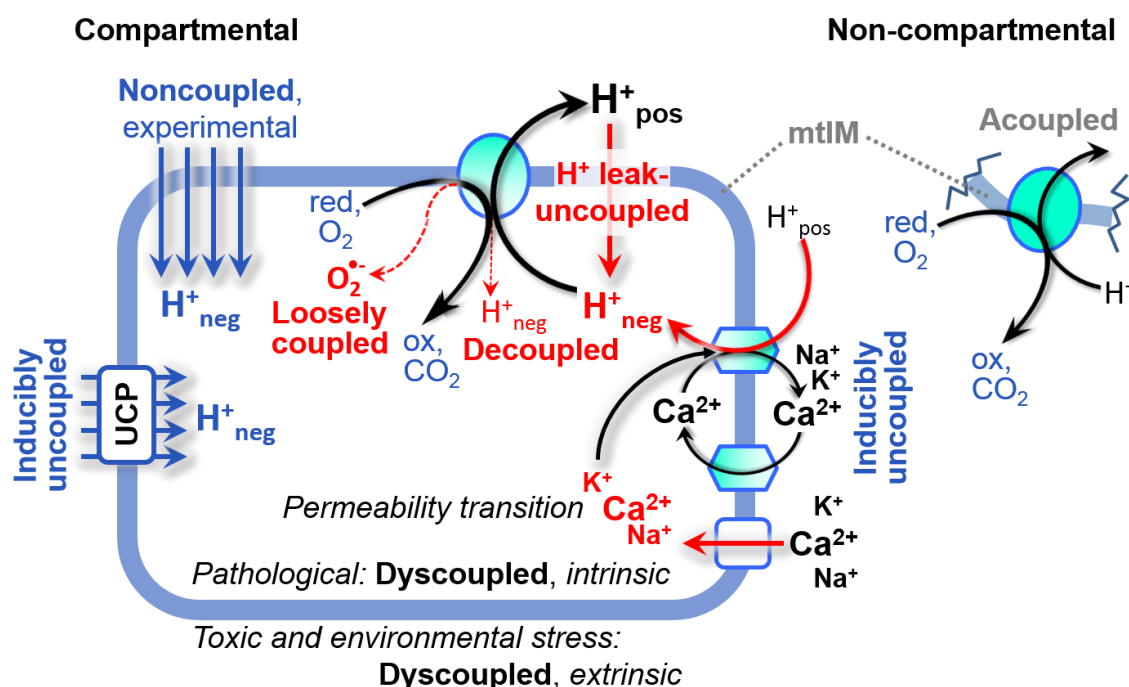
588 The H⁺_{pos}/O₂ coupling stoichiometry (referring to the full four electron reduction of O₂) depends on the
 589 relative involvement of the three coupling sites (respiratory Complexes CI, CIII and CIV) in the
 590 catabolic ET-pathway from reduced fuel substrates (electron donors) to the reduction of O₂ (electron
 591 acceptor). This varies with: (1) a bypass of CI by single or multiple electron input into the Q-junction;
 592 and (2) a bypass of CIV by involvement of alternative oxidases, AOX. AOX are expressed in all plants,
 593 some fungi, many protists, and several animal phyla, but are not expressed in vertebrate mitochondria
 594 (McDonald *et al.* 2009).

595 The H⁺_{pos}/O₂ coupling stoichiometry equals 12 in the ET-pathways involving CIII and CIV as
 596 proton pumps, increasing to 20 for the NADH-pathway through CI (**Figure 2B**), but a general consensus
 597 on H⁺_{pos}/O₂ stoichiometries remains to be reached (Hinkle 2005; Wikström and Hummer 2012; Sazanov

598 2015). The H^+_{neg}/P_{\gg} coupling stoichiometry (3.7; **Figure 2B**) is the sum of 2.7 H^+_{neg} required by the F-
 599 ATPase of vertebrate and most invertebrate species (Watt *et al.* 2010) and the proton balance in the
 600 translocation of ADP, ATP and P_i (**Figure 2C**). Taken together, the mechanistic P_{\gg}/O_2 ratio is calculated
 601 at 5.4 and 3.3 for NADH- and succinate-linked respiration, respectively (Eq. 1). The corresponding
 602 classical P_{\gg}/O ratios (referring to the 2 electron reduction of $0.5 O_2$) are 2.7 and 1.6 (Watt *et al.* 2010),
 603 in agreement with the measured P_{\gg}/O ratio for succinate of 1.58 ± 0.02 (Gnaiger *et al.* 2000).

604 **2.4.3. Uncoupling:** The effective P_{\gg}/O_2 flux ratio ($Y_{P_{\gg}/O_2} = J_{P_{\gg}}/J_{K_{O_2}}$) is diminished relative to the
 605 mechanistic P_{\gg}/O_2 ratio by intrinsic and extrinsic uncoupling or dyscoupling (**Figure 3**). Such
 606 generalized uncoupling is different from switching to mitochondrial pathways that involve fewer than
 607 three proton pumps ('coupling sites': Complexes CI, CIII and CIV), bypassing CI through multiple
 608 electron entries into the Q-junction, or CIII and CIV through AOX (**Figure 2B**). Reprogramming of
 609 mitochondrial pathways leading to different types of substrates being oxidized may be considered as a
 610 switch of gears (changing the stoichiometry by altering the substrate that is oxidized) rather than
 611 uncoupling (loosening the tightness of coupling relative to a fixed stoichiometry). In addition, Y_{P_{\gg}/O_2}
 612 depends on several experimental conditions of flux control, increasing as a hyperbolic function of [ADP]
 613 to a maximum value (Gnaiger 2001).

614



615

616

617 **Figure 3. Mechanisms of respiratory uncoupling**

618 An intact mitochondrial inner membrane, mtIM, is required for vectorial, compartmental coupling.
 619 'Acoupled' respiration is the consequence of structural disruption with catalytic activity of non-
 620 compartmental mitochondrial fragments. Inducible uncoupling, *e.g.*, by activation of UCP1, increases
 621 LEAK-respiration; experimentally noncoupled respiration provides an estimate of ET-capacity obtained
 622 by titration of protonophores stimulating respiration to maximum O_2 flux. H^+ leak-uncoupled,
 623 decoupled, and loosely coupled respiration are components of intrinsic uncoupling (**Table 2**).
 624 Pathological dysfunction may affect all types of uncoupling, including permeability transition (mtPT),
 625 causing intrinsically dyscoupled respiration. Similarly, toxicological and environmental stress factors
 626 can cause extrinsically dyscoupled respiration. Reduced fuel substrates, red; oxidized products, ox.

627 Uncoupling of mitochondrial respiration is a general term comprising diverse mechanisms:

- 628 1. Proton leak across the mtIM from the positive to the negative compartment (H^+ leak-uncoupled;
 629 **Figure 3**).
- 630 2. Cycling of other cations, strongly stimulated by mtPT; comparable to the use of protonophores,
 631 cation cycling is experimentally induced by valinomycin in the presence of K^+ ;
- 632 3. Decoupling by proton slip in the redox proton pumps when protons are effectively not pumped
 633 (CI, CIII and CIV) or are not driving phosphorylation (F-ATPase);

- 634 4. Loss of vesicular (compartmental) integrity when electron transfer is acoupled;
 635 5. Electron leak in the loosely coupled univalent reduction of O_2 to superoxide ($O_2^{\cdot-}$; superoxide
 636 anion radical).

637 Differences of terms—uncoupled *vs.* noncoupled—are easily overlooked, although they relate to
 638 different meanings of uncoupling (Figure 3 and Table 2).

639

640 2.5. Coupling states and respiratory rates

641

642 To extend the classical nomenclature on mitochondrial coupling states (Section 2.6) by a concept-
 643 driven terminology that explicitly incorporates information on the meaning of respiratory states, the
 644 terminology must be general and not restricted to any particular experimental protocol or mitochondrial
 645 preparation (Gnaiger 2009). Concept-driven nomenclature aims at mapping the meaning and concept
 646 behind the words and acronyms onto the forms of words and acronyms (Miller 1991). The focus of
 647 concept-driven nomenclature is primarily the conceptual *why*, along with clarification of the
 648 experimental *how*.

649

650 **Table 1. Coupling states and residual oxygen consumption in mitochondrial**
 651 **preparations in relation to respiration- and phosphorylation-flux, J_{kO_2} and $J_{P_{\gg}}$, and**
 652 **protonmotive force, pmf. Coupling states are established at kinetically-saturating**
 653 **concentrations of fuel substrates and O_2 .**

State	J_{kO_2}	$J_{P_{\gg}}$	pmf	Inducing factors	Limiting factors
LEAK	<i>L</i> ; low, cation leak-dependent respiration	0	max.	back-flux of cations including proton leak, proton slip	$J_{P_{\gg}} = 0$: (1) without ADP, <i>L</i> (n); (2) max. ATP/ADP ratio, <i>L</i> (T); or (3) inhibition of the phosphorylation-pathway, <i>L</i> (O _{my})
OXPHOS	<i>P</i> ; high, ADP-stimulated respiration, OXPHOS-capacity	max.	high	kinetically-saturating [ADP] and [P _i]	$J_{P_{\gg}}$ by phosphorylation-pathway capacity; or J_{kO_2} by ET-capacity
ET	<i>E</i> ; max., noncoupled respiration, ET-capacity	0	low	optimal external uncoupler concentration for max. $J_{O_2,E}$	J_{kO_2} by ET-capacity
ROX	<i>Rox</i> ; min., residual O_2 consumption	0	0	$J_{O_2,Rox}$ in non-ET-pathway oxidation reactions	inhibition of all ET-pathways; or absence of fuel substrates

654

655 To provide a diagnostic reference for respiratory capacities of core energy metabolism, the
 656 capacity of oxidative phosphorylation, OXPHOS, is measured at kinetically-saturating concentrations
 657 of ADP and P_i. The oxidative ET-capacity reveals the limitation of OXPHOS-capacity mediated by the
 658 phosphorylation-pathway. The ET- and phosphorylation-pathways comprise coupled segments of the
 659 OXPHOS-system. By application of external uncouplers, ET-capacity is measured as noncoupled
 660 respiration. The contribution of intrinsically uncoupled O_2 consumption is studied by preventing the
 661 stimulation of phosphorylation either in the absence of ADP or by inhibition of the phosphorylation-
 662 pathway. The corresponding states are collectively classified as LEAK-states when O_2 consumption
 663 compensates mainly for ion leaks, including the proton leak. Defined coupling states are induced by: (1)
 664 adding cation chelators such as EGTA, binding free Ca^{2+} and thus limiting cation cycling; (2) adding
 665 ADP and P_i; (3) inhibiting the phosphorylation-pathway; and (4) uncoupler titrations, while maintaining
 666 a defined ET-pathway state with constant fuel substrates and inhibitors of specific branches of the ET-
 667 pathway.

668 The three coupling states, ET, LEAK and OXPHOS, are shown schematically with the
 669 corresponding respiratory rates, abbreviated as E , L and P , respectively (**Figure 4**). We distinguish
 670 metabolic *pathways* from metabolic *states* and the corresponding metabolic *rates*; for example: ET-
 671 pathways, ET-states, and ET-capacities, E , respectively (**Table 1**). The protonmotive force is *high* in
 672 the OXPHOS-state when it drives phosphorylation, *maximum* in the LEAK-state of coupled
 673 mitochondria, driven by LEAK-respiration at a minimum back-flux of cations to the matrix side, and
 674 *very low* in the ET-state when uncouplers short-circuit the proton cycle (**Table 1**).

675
 676 **Figure 4. Four-compartment model of oxidative phosphorylation**
 677 Respiratory states (ET, OXPHOS, LEAK; **Table 1**) and corresponding
 678 rates (E , P , L) are connected by the protonmotive force, pmf. (1) ET-
 679 capacity, E , is partitioned into (2) dissipative LEAK-respiration, L ,
 680 when the Gibbs energy change of catabolic O_2 flux is irreversibly lost,
 681 (3) net OXPHOS-capacity, $P-L$, with partial conservation of the capacity to perform work, and (4) the excess capacity, $E-P$. Modified from Gnaiger (2014).

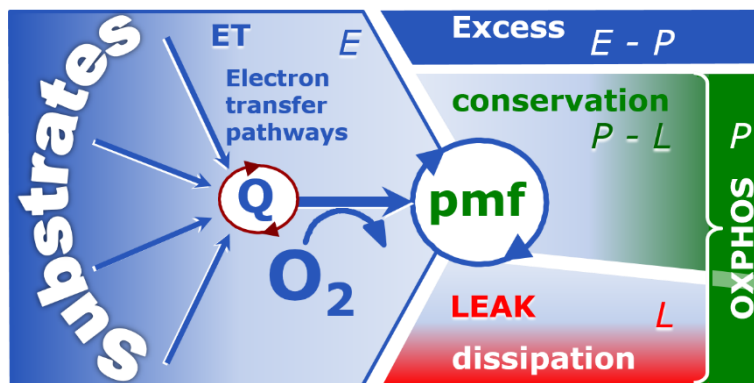
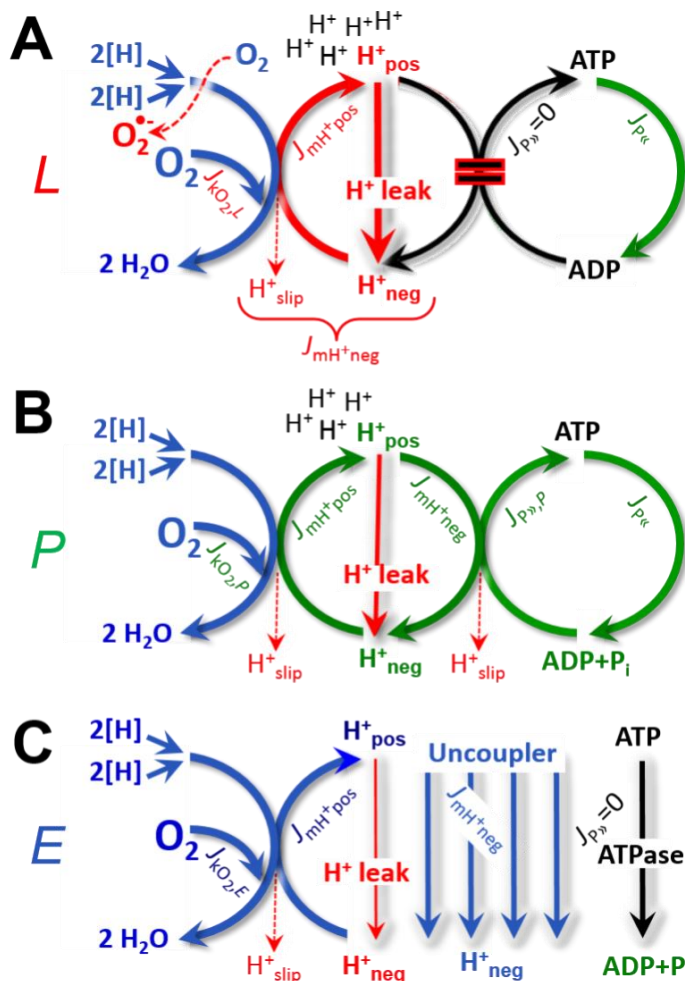


Figure 5. Respiratory coupling states

(A) **LEAK-state and rate, L** : Oxidation only, since phosphorylation is arrested, $J_{P\gg} = 0$, and catabolic O_2 flux, $J_{kO_2,L}$, is controlled mainly by the proton leak and slip, J_{mH^+neg} , at maximum protonmotive force (**Figure 4**). Extramitochondrial ATP may be hydrolyzed by extramitochondrial ATPases, $J_{P\ll}$; then phosphorylation must be blocked.

(B) **OXPHOS-state and rate, P** : Oxidation coupled to phosphorylation, $J_{P\gg}$, which is stimulated by kinetically-saturating [ADP] and $[P_i]$, supported by a high protonmotive force. O_2 flux, $J_{kO_2,P}$, is well-coupled at a $P\gg/O_2$ flux ratio of $J_{P\gg,P} \cdot J_{O_2,P}^{-1}$. Extramitochondrial ATPases may recycle ATP, $J_{P\ll}$.

(C) **ET-state and rate, E** : Oxidation only, since phosphorylation is zero, $J_{P\gg} = 0$, at optimum exogenous uncoupler concentration when noncoupled respiration, $J_{kO_2,E}$, is maximum. The F-ATPase may hydrolyze extramitochondrial ATP.



691 **2.5.1. LEAK-state (Figure 5A):** The LEAK-state is defined as a state of mitochondrial
 692 respiration when O₂ flux mainly compensates for ion leaks in the absence of ATP synthesis, at
 693 kinetically-saturating concentrations of O₂, respiratory fuel substrates and P_i. LEAK-respiration is
 694 measured to obtain an estimate of intrinsic uncoupling without addition of an experimental uncoupler:
 695 (1) in the absence of adenylates, *i.e.*, AMP, ADP and ATP; (2) after depletion of ADP at a maximum
 696 ATP/ADP ratio; or (3) after inhibition of the phosphorylation-pathway by inhibitors of F-ATPase—such
 697 as oligomycin, or of adenine nucleotide translocase—such as carboxyatractyloside. Adjustment of the
 698 nominal concentration of these inhibitors to the density of biological sample applied can minimize or
 699 avoid inhibitory side-effects exerted on ET-capacity or even some dyscoupling.
 700
 701

Table 2. Terms on respiratory coupling and uncoupling.

Term	J_{kO_2}	$P \gg O_2$	Notes	
acoupled		0	electron transfer in mitochondrial fragments without vectorial proton translocation (Figure 3)	
intrinsic, no protonophore added	uncoupled	L	0	non-phosphorylating LEAK-respiration (Figure 5A)
	proton leak-uncoupled		0	component of L , H ⁺ diffusion across the mtIM (Figure 3)
	decoupled		0	component of L , proton slip (Figure 3)
	loosely coupled		0	component of L , lower coupling due to superoxide formation and bypass of proton pumps by electron leak (Figure 3)
	dyscoupled		0	pathologically, toxicologically, environmentally increased uncoupling, mitochondrial dysfunction
	inducibly uncoupled		0	by UCP1 or cation (<i>e.g.</i> , Ca ²⁺) cycling (Figure 3)
noncoupled	E	0	ET-capacity, non-phosphorylating respiration stimulated to maximum flux at optimum exogenous protonophore concentration (Figure 5C)	
well-coupled	P	high	OXPPOS-capacity , phosphorylating respiration with an intrinsic LEAK component (Figure 5B)	
fully coupled	$P - L$	max.	OXPPOS-capacity corrected for LEAK-respiration (Figure 4)	

702

703

704

705

706

707

708

709

710

711

712

713

714

715

716

717

718

719

720

- **Proton leak and uncoupled respiration:** The intrinsic proton leak is the *uncoupled* leak current of protons in which protons diffuse across the mtIM in the dissipative direction of the downhill protonmotive force without coupling to phosphorylation (**Figure 5A**). The proton leak flux depends non-linearly on the protonmotive force (Garlid *et al.* 1989; Divakaruni and Brand 2011), which is a temperature-dependent property of the mtIM and may be enhanced due to possible contamination by free fatty acids. Inducible uncoupling mediated by uncoupling protein 1 (UCP1) is physiologically controlled, *e.g.*, in brown adipose tissue. UCP1 is a member of the mitochondrial carrier family that is involved in the translocation of protons across the mtIM (Jezek *et al.* 2018). Consequently, this short-circuit lowers the protonmotive force and stimulates electron transfer, respiration, and heat dissipation in the absence of phosphorylation of ADP.
- **Cation cycling:** There can be other cation contributors to leak current including calcium and probably magnesium. Calcium influx is balanced by mitochondrial Na⁺/Ca²⁺ or H⁺/Ca²⁺ exchange, which is balanced by Na⁺/H⁺ or K⁺/H⁺ exchanges. This is another effective uncoupling mechanism different from proton leak (**Table 2**).
- **Proton slip and decoupled respiration:** Proton slip is the *decoupled* process in which protons are only partially translocated by a redox proton pump of the ET-pathways and slip back to the original vesicular compartment. The proton leak is the dominant contributor to the overall leak current in mammalian mitochondria incubated under physiological conditions at 37 °C, whereas

721 proton slip increases at lower experimental temperature (Canton *et al.* 1995). Proton slip can also
 722 happen in association with the F-ATPase, in which the proton slips downhill across the pump to
 723 the matrix without contributing to ATP synthesis. In each case, proton slip is a property of the
 724 proton pump and increases with the pump turnover rate.

- 725 • **Electron leak and loosely coupled respiration:** Superoxide production by the ETS leads to a
 726 bypass of redox proton pumps and correspondingly lower P_{H}/O_2 ratio. This depends on the actual
 727 site of electron leak and the scavenging of hydrogen peroxide by cytochrome *c*, whereby electrons
 728 may re-enter the ETS with proton translocation by CIV.
- 729 • **Loss of compartmental integrity and acoupled respiration:** Electron transfer and catabolic O_2
 730 flux proceed without compartmental proton translocation in disrupted mitochondrial fragments.
 731 Such fragments are an artefact of mitochondrial isolation, and may not fully fuse to re-establish
 732 structurally intact mitochondria. Loss of mtIM integrity, therefore, is the cause of acoupled
 733 respiration, which is a nonvectorial dissipative process without control by the protonmotive force.
- 734 • **Dyscoupled respiration:** Mitochondrial injuries may lead to *dyscoupling* as a pathological or
 735 toxicological cause of *uncoupled* respiration. Dyscoupling may involve any type of uncoupling
 736 mechanism, *e.g.*, opening the mtPT pore. Dyscoupled respiration is distinguished from the
 737 experimentally induced *noncoupled* respiration in the ET-state (**Table 2**).

738
 739 **2.5.2. OXPHOS-state (Figure 5B):** The OXPHOS-state is defined as the respiratory state with
 740 kinetically-saturating concentrations of O_2 , respiratory and phosphorylation substrates, and absence of
 741 exogenous uncoupler, which provides an estimate of the maximal respiratory capacity in the OXPHOS-
 742 state for any given ET-pathway state. Respiratory capacities at kinetically-saturating substrate
 743 concentrations provide reference values or upper limits of performance, aiming at the generation of data
 744 sets for comparative purposes. Physiological activities and effects of substrate kinetics can be evaluated
 745 relative to the OXPHOS-capacity.

746 As discussed previously, 0.2 mM ADP does not fully saturate flux in isolated mitochondria
 747 (Gnaiger 2001; Puchowicz *et al.* 2004); greater [ADP] is required, particularly in permeabilized muscle
 748 fibres and cardiomyocytes, to overcome limitations by intracellular diffusion and by the reduced
 749 conductance of the mtOM (Jepihhina *et al.* 2011; Illaste *et al.* 2012; Simson *et al.* 2016), either through
 750 interaction with tubulin (Rostovtseva *et al.* 2008) or other intracellular structures (Birkedal *et al.* 2014).
 751 In addition, saturating ADP concentrations need to be evaluated under different experimental conditions
 752 such as temperature (Lemieux *et al.* 2017) and with different animal models (Blier and Guderley, 1993).
 753 In permeabilized muscle fibre bundles of high respiratory capacity, the apparent K_m for ADP increases
 754 up to 0.5 mM (Saks *et al.* 1998), consistent with experimental evidence that >90% saturation is reached
 755 only at >5 mM ADP (Pesta and Gnaiger 2012). Similar ADP concentrations are also required for
 756 accurate determination of OXPHOS-capacity in human clinical cancer samples and permeabilized cells
 757 (Klepinin *et al.* 2016; Koit *et al.* 2017). 2.5 to 5 mM ADP is sufficient to obtain the actual OXPHOS-
 758 capacity in many types of permeabilized tissue and cell preparations, but experimental validation is
 759 required in each specific case.

760 **2.5.3. Electron transfer-state (Figure 5C):** O_2 flux determined in the ET-state yields an estimate
 761 of ET-capacity. The ET-state is defined as the *noncoupled* state with kinetically-saturating
 762 concentrations of O_2 , respiratory substrate and optimum exogenous uncoupler concentration for
 763 maximum O_2 flux. Uncouplers are weak lipid-soluble acids which function as protonophores. These
 764 disrupt the barrier function of the mtIM and thus short circuit the protonmotive system, functioning like
 765 a clutch in a mechanical system. As a consequence of the nearly collapsed protonmotive force, the
 766 driving force is insufficient for phosphorylation, and $J_{P_{\text{H}}} = 0$. The most frequently used uncouplers are
 767 carbonyl cyanide *m*-chloro phenyl hydrazone (CCCP), carbonyl cyanide *p*-
 768 trifluoromethoxyphenylhydrazone (FCCP), or dinitrophenol (DNP). Stepwise titration of uncouplers
 769 stimulates respiration up to or above the level of O_2 consumption rates in the OXPHOS-state; respiration
 770 is inhibited, however, above optimum uncoupler concentrations (Mitchell 2011). Data obtained with a
 771 single dose of uncoupler must be evaluated with caution, particularly when a fixed uncoupler
 772 concentration is used in studies exploring a treatment or disease that may alter the mitochondrial content
 773 or mitochondrial sensitivity to inhibition by uncouplers. There is a need for new protonophoric
 774 uncouplers that drive maximal respiration across a broad dosing range and do not inhibit respiration at
 775 high concentrations (Kenwood *et al.* 2013). The effect on ET-capacity of the reversed function of F-
 776 ATPase ($J_{P_{\text{H}}}$; **Figure 5C**) can be evaluated in the presence and absence of extramitochondrial ATP.

777 **2.5.4. ROX state and *Rox*:** Besides the three fundamental coupling states of mitochondrial
 778 preparations, the state of residual O₂ consumption, ROX, which although not a coupling state, is relevant
 779 to assess respiratory function (**Figure 1**). The rate of residual oxygen consumption, *Rox*, is defined as
 780 O₂ consumption due to oxidative reactions measured after inhibition of ET with rotenone, malonic acid
 781 and antimycin A. Cyanide and azide inhibit not only CIV but catalase and several peroxidases involved
 782 in *Rox*. High concentrations of antimycin A, but not rotenone or cyanide, inhibit peroxisomal acyl-CoA
 783 oxidase and D-amino acid oxidase (Vamecq *et al.* 1987). *Rox* represents a baseline used to correct
 784 respiration measured in defined coupling control states. *Rox*-corrected *L*, *P* and *E* not only lower the
 785 values of total fluxes, but also change the flux control ratios *L/P* and *L/E*. *Rox* is not necessarily
 786 equivalent to non-mitochondrial reduction of O₂, considering O₂-consuming reactions in mitochondria
 787 that are not related to ET—such as O₂ consumption in reactions catalyzed by monoamine oxidases (type
 788 A and B), monooxygenases (cytochrome P450 monooxygenases), dioxygenase (sulfur dioxygenase and
 789 trimethyllysine dioxygenase), and several hydroxylases. Even isolated mitochondrial fractions,
 790 especially those obtained from liver, may be contaminated by peroxisomes, as shown by transmission
 791 electron microscopy. This fact makes the exact determination of mitochondrial O₂ consumption and
 792 mitochondria-associated generation of reactive oxygen species complicated (Schönfeld *et al.* 2009;
 793 Speijer 2016; **Figure 2**). The dependence of ROX-linked O₂ consumption needs to be studied in detail
 794 together with non-ET enzyme activities, availability of specific substrates, O₂ concentration, and
 795 electron leakage leading to the formation of reactive oxygen species.

796 **2.5.5. Quantitative relations:** *E* may exceed or be equal to *P*. $E > P$ is observed in many types
 797 of mitochondria, varying between species, tissues and cell types (Gnaiger 2009). *E-P* is the excess ET-
 798 capacity pushing the phosphorylation-flux (**Figure 2C**) to the limit of its capacity for utilizing the
 799 protonmotive force. In addition, the magnitude of *E-P* depends on the tightness of respiratory coupling
 800 or degree of uncoupling, since an increase of *L* causes *P* to increase towards the limit of *E*. The *excess*
 801 *E-P* capacity, *E-P*, therefore, provides a sensitive diagnostic indicator of specific injuries of the
 802 phosphorylation-pathway, under conditions when *E* remains constant but *P* declines relative to controls
 803 (**Figure 4**). Substrate cocktails supporting simultaneous convergent electron transfer to the Q-junction
 804 for reconstitution of TCA cycle function establish pathway control states with high ET-capacity, and
 805 consequently increase the sensitivity of the *E-P* assay.

806 *E* cannot theoretically be lower than *P*. $E < P$ must be discounted as an artefact, which may be
 807 caused experimentally by: (1) loss of oxidative capacity during the time course of the respirometric
 808 assay, since *E* is measured subsequently to *P*; (2) using insufficient uncoupler concentrations; (3) using
 809 high uncoupler concentrations which inhibit ET (Gnaiger 2008); (4) high oligomycin concentrations
 810 applied for measurement of *L* before titrations of uncoupler, when oligomycin exerts an inhibitory effect
 811 on *E*. On the other hand, the excess ET-capacity is overestimated if non-saturating [ADP] or [P_i] are
 812 used. See State 3 in the next section.

813 The net OXPHOS-capacity is calculated by subtracting *L* from *P* (**Figure 4**). The net P_»/O₂ equals
 814 $P_{»}/(P-L)$, wherein the dissipative LEAK component in the OXPHOS-state may be overestimated. This
 815 can be avoided by measuring LEAK-respiration in a state when the protonmotive force is adjusted to its
 816 slightly lower value in the OXPHOS-state by titration of an ET inhibitor (Divakaruni and Brand 2011).
 817 Any turnover-dependent components of proton leak and slip, however, are underestimated under these
 818 conditions (Garlid *et al.* 1993). In general, it is inappropriate to use the term *ATP production* or *ATP*
 819 *turnover* for the difference of O₂ flux measured in the OXPHOS and LEAK states. *P-L* is the upper limit
 820 of OXPHOS-capacity that is freely available for ATP production (corrected for LEAK-respiration) and
 821 is fully coupled to phosphorylation with a maximum mechanistic stoichiometry (**Figure 4**).

822 LEAK-respiration and OXPHOS-capacity depend on (1) the tightness of coupling under the
 823 influence of the respiratory uncoupling mechanisms (**Figure 3**), and (2) the coupling stoichiometry,
 824 which varies as a function of the substrate type undergoing oxidation in ET-pathways with either two
 825 or three coupling sites (**Figure 2B**). When cocktails with NADH-linked substrates and succinate are
 826 used, the relative contribution of ET-pathways with three or two coupling sites cannot be controlled
 827 experimentally, is difficult to determine, and may shift in transitions between LEAK-, OXPHOS- and
 828 ET-states (Gnaiger 2014). Under these experimental conditions, we cannot separate the tightness of
 829 coupling *versus* coupling stoichiometry as the mechanisms of respiratory control in the shift of *L/P*
 830 ratios. The tightness of coupling and fully coupled O₂ flux, *P-L* (**Table 2**), therefore, are obtained from
 831 measurements of coupling control of LEAK-respiration, OXPHOS- and ET-capacities in well-defined

832 pathway states, using either pyruvate and malate as substrates or the classical succinate and rotenone
833 substrate-inhibitor combination (**Figure 2B**).

834 **2.5.6. The steady-state:** Mitochondria represent a thermodynamically open system in non-
835 equilibrium states of biochemical energy transformation. State variables (protonmotive force; redox
836 states) and metabolic *rates* (fluxes) are measured in defined mitochondrial respiratory *states*. Steady-
837 states can be obtained only in open systems, in which changes by internal transformations, *e.g.*, O₂
838 consumption, are instantaneously compensated for by external fluxes across the system boundary, *e.g.*,
839 O₂ supply, preventing a change of O₂ concentration in the system (Gnaiger 1993b). Mitochondrial
840 respiratory states monitored in closed systems satisfy the criteria of pseudo-steady states for limited
841 periods of time, when changes in the system (concentrations of O₂, fuel substrates, ADP, P_i, H⁺) do not
842 exert significant effects on metabolic fluxes (respiration, phosphorylation). Such pseudo-steady states
843 require respiratory media with sufficient buffering capacity and substrates maintained at kinetically-
844 saturating concentrations, and thus depend on the kinetics of the processes under investigation.

846 2.6. Classical terminology for isolated mitochondria

847 *'When a code is familiar enough, it ceases appearing like a code; one forgets that there is a*
848 *decoding mechanism. The message is identical with its meaning'* (Hofstadter 1979).

850 Chance and Williams (1955; 1956) introduced five classical states of mitochondrial respiration
851 and cytochrome redox states. **Table 3** shows a protocol with isolated mitochondria in a closed
852 respirometric chamber, defining a sequence of respiratory states. States and rates are not specifically
853 distinguished in this nomenclature.

854
855 **Table 3. Metabolic states of mitochondria (Chance and**
856 **Williams, 1956; Table V).**

State	[O ₂]	ADP level	Substrate level	Respiration rate	Rate-limiting substance
1	>0	low	low	slow	ADP
2	>0	high	~0	slow	substrate
3	>0	high	high	fast	respiratory chain
4	>0	low	high	slow	ADP
5	0	high	high	0	oxygen

858
859 **2.6.1. State 1** is obtained after addition of isolated mitochondria to air-saturated
860 isoosmotic/isotonic respiration medium containing P_i, but no fuel substrates and no adenylates.

861 **2.6.2. State 2** is induced by addition of a 'high' concentration of ADP (typically 100 to 300 μM),
862 which stimulates respiration transiently on the basis of endogenous fuel substrates and phosphorylates
863 only a small portion of the added ADP. State 2 is then obtained at a low respiratory activity limited by
864 exhausted endogenous fuel substrate availability (**Table 3**). If addition of specific inhibitors of
865 respiratory complexes such as rotenone does not cause a further decline of O₂ flux, State 2 is equivalent
866 to the ROX state (See below.). If inhibition is observed, undefined endogenous fuel substrates are a
867 confounding factor of pathway control, contributing to the effect of subsequently externally added
868 substrates and inhibitors. In contrast to the original protocol, an alternative sequence of titration steps is
869 frequently applied, in which the alternative 'State 2' has an entirely different meaning when this second
870 state is induced by addition of fuel substrate without ADP or ATP (LEAK-state; in contrast to State 2
871 defined in **Table 1** as a ROX state). Some researchers have called this condition as 'pseudostate 4'
872 because it has no significant concentrations of adenine nucleotides and hence it is not a near-
873 physiological condition, although it should be used for calculating the net OXPHOS-capacity, *P-L*.

874 **2.6.3. State 3** is the state stimulated by addition of fuel substrates while the ADP concentration
875 is still high (**Table 3**) and supports coupled energy transformation through oxidative phosphorylation.
876 'High ADP' is a concentration of ADP specifically selected to allow the measurement of State 3 to State
877 4 transitions of isolated mitochondria in a closed respirometric chamber. Repeated ADP titration re-
878 establishes State 3 at 'high ADP'. Starting at O₂ concentrations near air-saturation (193 or 238 μM O₂

879 at 37 °C or 25 °C and sea level at 1 atm or 101.32 kPa, and an oxygen solubility of respiration medium
 880 at 0.92 times that of pure water; Forstner and Gnaiger 1983), the total ADP concentration added must
 881 be low enough (typically 100 to 300 μM) to allow phosphorylation to ATP at a coupled O_2 flux that
 882 does not lead to O_2 depletion during the transition to State 4. In contrast, kinetically-saturating ADP
 883 concentrations usually are 10-fold higher than 'high ADP', e.g., 2.5 mM in isolated mitochondria. The
 884 abbreviation State 3u is occasionally used in bioenergetics, to indicate the state of respiration after
 885 titration of an uncoupler, without sufficient emphasis on the fundamental difference between OXPHOS-
 886 capacity (*well-coupled* with an endogenous uncoupled component) and ET-capacity (*noncoupled*).

887 **2.6.4. State 4** is a LEAK-state that is obtained only if the mitochondrial preparation is intact and
 888 well-coupled. Depletion of ADP by phosphorylation to ATP causes a decline of O_2 flux in the transition
 889 from State 3 to State 4. Under the conditions of State 4, a maximum protonmotive force and high
 890 ATP/ADP ratio are maintained. The gradual decline of Y_{P}/O_2 towards diminishing [ADP] at State 4 must
 891 be taken into account for calculation of P/O_2 ratios (Gnaiger 2001). State 4 respiration, L_T (**Table 1**),
 892 reflects intrinsic proton leak and ATP hydrolysis activity. O_2 flux in State 4 is an overestimation of
 893 LEAK-respiration if the contaminating ATP hydrolysis activity recycles some ATP to ADP, J_{P_s} , which
 894 stimulates respiration coupled to phosphorylation, $J_{\text{P}_s} > 0$. Some degree of mechanical disruption and
 895 loss of mitochondrial integrity allows the exposed mitochondrial F-ATPases to hydrolyze the ATP
 896 synthesized by the fraction of coupled mitochondria. This can be tested by inhibition of the
 897 phosphorylation-pathway using oligomycin, ensuring that $J_{\text{P}_s} = 0$ (State 4o). On the other hand, the State
 898 4 respiration reached after exhaustion of added ADP is a more physiological condition, i.e., presence of
 899 ATP, ADP and even AMP. Sequential ADP titrations re-establish State 3, followed by State 3 to State
 900 4 transitions while sufficient O_2 is available. Anoxia may be reached, however, before exhaustion of
 901 ADP (State 5).

902 **2.6.5. State 5** 'may be obtained by antimycin A treatment or by anaerobiosis' (Chance and
 903 Williams, 1955) 'These definitions give State 5 two different meanings of ROX or anoxia, respectively.
 904 Anoxia is obtained after exhaustion of O_2 in a closed respirometric chamber. Diffusion of O_2 from the
 905 surroundings into the aqueous solution may be a confounding factor preventing complete anoxia
 906 (Gnaiger 2001).

907 In **Table 3**, only States 3 and 4 are coupling control states, with the restriction that rates in State
 908 3 may be limited kinetically by non-saturating ADP concentrations.

910 2.7. Control and regulation

911 The terms metabolic *control* and *regulation* are frequently used synonymously, but are
 912 distinguished in metabolic control analysis: "We could understand the regulation as the mechanism that
 913 occurs when a system maintains some variable constant over time, in spite of fluctuations in external
 914 conditions (homeostasis of the internal state). On the other hand, metabolic control is the power to
 915 change the state of the metabolism in response to an external signal" (Fell 1997). Respiratory control
 916 may be induced by experimental control signals that exert an influence on: (1) ATP demand and ADP
 917 phosphorylation-rate; (2) fuel substrate composition, pathway competition; (3) available amounts of
 918 substrates and O_2 , e.g., starvation and hypoxia; (4) the protonmotive force, redox states, flux-force
 919 relationships, coupling and efficiency; (5) Ca^{2+} and other ions including H^+ ; (6) inhibitors, e.g., nitric
 920 oxide or intermediary metabolites such as oxaloacetate; (7) signalling pathways and regulatory proteins,
 921 e.g., insulin resistance, transcription factor hypoxia inducible factor 1.

922 Mechanisms of respiratory control and regulation include adjustments of: (1) enzyme activities
 923 by allosteric mechanisms and phosphorylation; (2) enzyme content, concentrations of cofactors and
 924 conserved moieties such as adenylates, nicotinamide adenine dinucleotide [NAD^+/NADH], coenzyme
 925 Q, cytochrome *c*; (3) metabolic channeling by supercomplexes; and (4) mitochondrial density (enzyme
 926 concentrations and membrane area) and morphology (cristae folding, fission and fusion). Mitochondria
 927 are targeted directly by hormones, e.g., progesterone and glucocorticoids, which affect their energy
 928 metabolism (Lee *et al.* 2013; Gerö and Szabo 2016; Price and Dai 2016; Moreno *et al.* 2017; Singh *et*
 929 *al.* 2018). Evolutionary or acquired differences in the genetic and epigenetic basis of mitochondrial
 930 function (or dysfunction) between individuals; age; biological sex, and hormone concentrations; life
 931 style including exercise and nutrition; and environmental issues including thermal, atmospheric, toxic
 932 and pharmacological factors, exert an influence on all control mechanisms listed above. For reviews,
 933 see Brown 1992; Gnaiger 1993a, 2009; 2014; Paradies *et al.* 2014; Morrow *et al.* 2017.

Lack of control by a metabolic pathway, *e.g.*, phosphorylation-pathway, means that there will be no response to a variable activating it, *e.g.*, [ADP]. The reverse, however, is not true as the absence of a response to [ADP] does not exclude the phosphorylation-pathway from having some degree of control. The degree of control of a component of the OXPHOS-pathway on an output variable, such as O₂ flux, will in general be different from the degree of control on other outputs, such as phosphorylation-flux or proton leak flux. Therefore, it is necessary to be specific as to which input and output are under consideration (Fell 1997).

Respiratory control refers to the ability of mitochondria to adjust O₂ flux in response to external control signals by engaging various mechanisms of control and regulation. Respiratory control is monitored in a mitochondrial preparation under conditions defined as respiratory states, preferentially under near-physiological conditions of temperature, pH, and medium ionic composition, to generate data of higher biological relevance. When phosphorylation of ADP to ATP is stimulated or depressed, an increase or decrease is observed in electron transfer measured as O₂ flux in respiratory coupling states of intact mitochondria ('controlled states' in the classical terminology of bioenergetics). Alternatively, coupling of electron transfer with phosphorylation is diminished by uncouplers. The corresponding coupling control state is characterized by a high respiratory rate without control by P» (noncoupled or 'uncontrolled state').

3. What is a rate?

The term *rate* is not adequately defined to be useful for reporting data. Normalization of 'rates' leads to a diversity of formats. Application of common and defined units is required for direct transfer of reported results into a database. The second [s] is the SI unit for the base quantity *time*. It is also the standard time-unit used in solution chemical kinetics.

The inconsistency of the meanings of rate becomes apparent when considering Galileo Galilei's famous principle, that 'bodies of different weight all fall at the same rate (have a constant acceleration)' (Coopersmith 2010). A rate may be an extensive quantity, which is a *flow*, *I*, when expressed per object (per number of cells or organisms) or per chamber (per system). 'System' is defined as the open or closed chamber of the measuring device. A rate is a *flux*, *J*, when expressed as a size-specific quantity (Figure 6A; Box 2).

- **Extensive quantities:** An extensive quantity increases proportionally with system size. For example, mass and volume are extensive quantities. Flow is an extensive quantity. The magnitude of an extensive quantity is completely additive for non-interacting subsystems. The magnitude of these quantities depends on the extent or size of the system (Cohen *et al.* 2008).
- **Size-specific quantities:** 'The adjective *specific* before the name of an extensive quantity is often used to mean *divided by mass*' (Cohen *et al.* 2008). In this system-paradigm, mass-specific flux is flow divided by mass of the system (the total mass of everything within the measuring chamber or reactor). Rates are frequently expressed as volume-specific flux. A mass-specific or volume-specific quantity is independent of the extent of non-interacting homogenous subsystems. Tissue-specific quantities (related to the *sample* in contrast to the *system*) are of fundamental interest in the field of comparative mitochondrial physiology, where *specific* refers to the *type of the sample* rather than *mass of the system*. The term *specific*, therefore, must be clarified; *sample-specific*, *e.g.*, muscle mass-specific normalization, is distinguished from *system-specific* quantities (mass or volume; Figure 6).
- **Intensive quantities:** In contrast to size-specific properties, forces are intensive quantities defined as the change of an extensive quantity per advancement of an energy transformation (Gnaiger 1993b).
- **Formats:** The quantity of a sample *X* can be expressed in different formats. n_X , N_X , and m_X are the molar amount, number, and mass of *X*, respectively. When different formats are indicated in symbols of derived quantities, the format (\underline{n} , \underline{N} , \underline{m}) is shown as a subscript (*underlined italic*), as in $I_{O_2/\underline{N}X}$ and $J_{O_2/\underline{m}X}$. Oxygen flow and flux are expressed in the molar format, n_{O_2} [mol], but in the volume format, V_{O_2} [m³] in ergometry. For mass-specific flux these formats can be distinguished as $J_{\underline{n}O_2/\underline{m}X}$ and $J_{\underline{V}O_2/\underline{m}X}$, respectively. Further examples are given in Figure 6 and Table 4.

991

992

Figure 6. Flow and flux, and normalization in structure-function analysis

993

994

995

996

997

998

999

1000

1001

1002

1003

1004

1005

1006

1007

1008

1009

1010

1011

1012

1013

1014

1015

1016

1017

1018

1019

1020

1021

1022

1023

1024

1025

1026

1027

1028

1029

1030

1031

1032

1033

1034

1035

1036

1037

1038

1039

1040

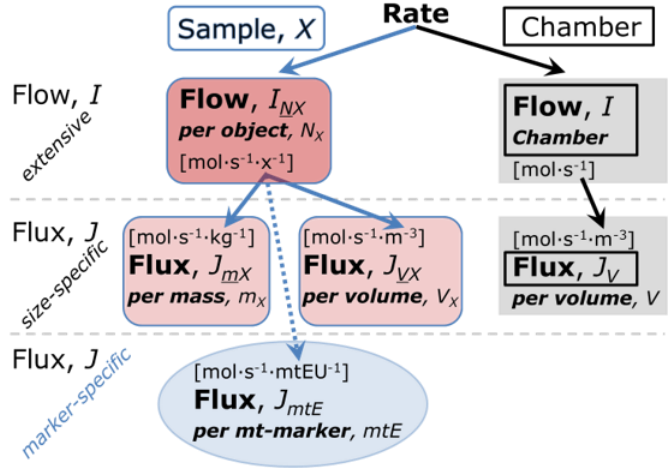
1041

1042

1043

1044

A



B

$$\begin{aligned}
 \text{Flow per cell} &= \text{mt-specific Flux} \times \text{mt-Density} \times \text{Mass per cell} \\
 I_{O_2/Nce} &= \underbrace{J_{O_2/CS}}_{\text{mol}\cdot\text{s}^{-1}} \cdot \underbrace{D_{CS}}_{\text{IU/kg}} \cdot M_{ce} \\
 \frac{\text{mol}\cdot\text{s}^{-1}}{x} &= \frac{\text{mol}\cdot\text{s}^{-1}}{\text{IU}} \cdot \frac{\text{IU}}{\text{kg}} \cdot \frac{\text{kg}}{x} \\
 \text{Size} & \\
 \text{Flow per cell} &= \text{Mass-specific Flux } J_{O_2/Mce} \times \text{Mass per cell} \\
 \text{Structure} & \\
 \text{Flow per cell} &= \text{mt-specific Flux} \times \text{mt-Content per cell } CS_{Nce} \\
 I_{O_2/Nce} &= J_{O_2/CS} \cdot \underbrace{D_{CS} \cdot M_{ce}}_{\text{IU/kg} \cdot \text{kg}} \\
 \frac{\text{mol}\cdot\text{s}^{-1}}{x} &= \frac{\text{mol}\cdot\text{s}^{-1}}{\text{IU}} \cdot \frac{\text{IU}}{\text{kg}} \cdot \frac{\text{kg}}{x} \\
 \text{Aerobic cell performance} &= \begin{cases} \text{mt-Quality} \times \text{mt-Quantity} \\ \text{mt-Function} \times \text{mt-Structure} \end{cases}
 \end{aligned}$$

Box 2: Metabolic flows and fluxes: vectorial, vectorial, and scalar

In a generalization of electrical terms, flow as an extensive quantity (I ; per system) is distinguished from flux as a size-specific quantity (J ; per system size). *Flows*, I_{tr} , are defined for all transformations as extensive quantities. Electric charge per unit time is electric flow or current, $I_{el} = dQ_{el} \cdot dt^{-1}$ [$A \equiv C \cdot s^{-1}$]. When dividing I_{el} by size of the system (cross-sectional area of a ‘wire’), we obtain flux as a size-specific quantity, which is the current density (surface-density of flow) perpendicular to the direction of flux, $J_{el} = I_{el} \cdot A^{-1}$ [$A \cdot m^{-2}$] (Cohen et al. 2008). Fluxes with *spatial* geometric direction and magnitude are *vectors*. Vector and scalar *fluxes* are related to flows as $J_{tr} = I_{tr} \cdot A^{-1}$ [$\text{mol} \cdot \text{s}^{-1} \cdot \text{m}^{-2}$] and $J_{tr} = I_{tr} \cdot V^{-1}$ [$\text{mol} \cdot \text{s}^{-1} \cdot \text{m}^{-3}$], expressing flux as an area-specific vector or volume-specific vectorial or scalar quantity, respectively (Gnaiger 1993b). We use the metre–kilogram–second–ampere (MKSA) international system of units (SI) for general cases ([m], [kg], [s] and [A]), with decimal SI prefixes for specific applications (Table 4).

We suggest defining: (1) *vectorial* fluxes, which are translocations as functions of *gradients* with direction in geometric space in continuous systems; (2) *vectorial* fluxes, which describe translocations in discontinuous systems and are restricted to information on *compartmental differences*

1045 (transmembrane proton flux); and (3) *scalar fluxes*, which are transformations in a *homogenous system*
 1046 (catabolic O₂ flux, J_{kO_2}).

1047 4. Normalization of rate per sample

1048

1049 The challenges of measuring mitochondrial respiratory flux are matched by those of
 1050 normalization. Normalization (**Table 4**) is guided by physicochemical principles, methodological
 1051 considerations, and conceptual strategies (**Figure 6**).

1052

1053 **Table 4. Sample concentrations and normalization of flux.**

1054

Expression	Symbol	Definition	Unit	Notes
Sample				
identity of sample	X	object: cell, tissue, animal, patient		
number of sample entities X	N_X	number of objects	x	1
mass of sample X	m_X		kg	2
mass of object X	M_X	$M_X = m_X \cdot N_X^{-1}$	kg·x ⁻¹	2
Mitochondria				
mitochondria	mt	$X = mt$		
amount of mt-elementary components	mtE	quantity of mt-marker	mtEU	
Concentrations				
object number concentration	C_{NX}	$C_{NX} = N_X \cdot V^{-1}$	x·m ⁻³	3
sample mass concentration	C_{mX}	$C_{mX} = m_X \cdot V^{-1}$	kg·m ⁻³	
mitochondrial concentration	C_{mtE}	$C_{mtE} = mtE \cdot V^{-1}$	mtEU·m ⁻³	4
specific mitochondrial density	D_{mtE}	$D_{mtE} = mtE \cdot m_X^{-1}$	mtEU·kg ⁻¹	5
mitochondrial content, mtE per object X	mtE_{NX}	$mtE_{NX} = mtE \cdot N_X^{-1}$	mtEU·x ⁻¹	6
O₂ flow and flux				
flow, system	I_{O_2}	internal flow	mol·s ⁻¹	8
volume-specific flux	J_{V,O_2}	$J_{V,O_2} = I_{O_2} \cdot V^{-1}$	mol·s ⁻¹ ·m ⁻³	9
flow per object X	$I_{O_2/NX}$	$I_{O_2/NX} = J_{V,O_2} \cdot C_{NX}^{-1}$	mol·s ⁻¹ ·x ⁻¹	10
mass-specific flux	$J_{O_2/mX}$	$J_{O_2/mX} = J_{V,O_2} \cdot C_{mX}^{-1}$	mol·s ⁻¹ ·kg ⁻¹	
mt-marker-specific flux	$J_{O_2/mtE}$	$J_{O_2/mtE} = J_{V,O_2} \cdot C_{mtE}^{-1}$	mol·s ⁻¹ ·mtEU ⁻¹	11

1055 1 The unit x for a number is not used by IUPAC. To avoid confusion, the units [kg·x⁻¹] and [kg]
 1056 distinguish the mass per object from the mass of a sample that may contain any number of objects.
 1057 Similarly, the units for flow per system *versus* flow per object are [mol·s⁻¹] (Note 8) and [mol·s⁻¹·x⁻¹]
 1058 (Note 10).

1059 2 Units are given in the MKSA system (**Box 2**). The SI prefix k is used for the SI base unit of mass (kg
 1060 = 1,000 g). In praxis, various SI prefixes are used for convenience, to make numbers easily readable,
 1061 e.g., 1 mg tissue, cell or mitochondrial mass instead of 0.000001 kg.

1062 3 In case of cells (sample $X = \text{cells}$), the object number concentration is $C_{Nce} = N_{ce} \cdot V^{-1}$, and volume
 1063 may be expressed in [dm³ ≡ L] or [cm³ = mL]. See **Table 5** for different object types.

1064 4 mt-concentration is an experimental variable, dependent on sample concentration: (1) $C_{mtE} = mtE \cdot V^{-1}$;
 1065 (2) $C_{mtE} = mtE_X \cdot C_{NX}$; (3) $C_{mtE} = C_{mX} \cdot D_{mtE}$.

1066 5 If the amount of mitochondria, mtE , is expressed as mitochondrial mass, then D_{mtE} is the mass
 1067 fraction of mitochondria in the sample. If mtE is expressed as mitochondrial volume, V_{mt} , and the
 1068 mass of sample, m_X , is replaced by volume of sample, V_X , then D_{mtE} is the volume fraction of
 1069 mitochondria in the sample.

1070 6 $mtE_{NX} = mtE \cdot N_X^{-1} = C_{mtE} \cdot C_{NX}^{-1}$.

- 1071 7 O₂ can be replaced by other chemicals to study different reactions, e.g., ATP, H₂O₂, or vesicular
 1072 compartmental translocations, e.g., Ca²⁺.
 1073 8 I_{O₂} and V are defined per instrument chamber as a system of constant volume (and constant
 1074 temperature), which may be closed or open. I_{O₂} is abbreviated for I_{rO₂}, i.e., the metabolic or internal
 1075 O₂ flow of the chemical reaction r in which O₂ is consumed, hence the negative stoichiometric
 1076 number, $\nu_{O_2} = -1$. $I_{rO_2} = d_r n_{O_2} / dt \cdot \nu_{O_2}^{-1}$. If r includes all chemical reactions in which O₂ participates, then
 1077 $d_r n_{O_2} = dn_{O_2} - d_e n_{O_2}$, where dn_{O_2} is the change in the amount of O₂ in the instrument chamber and $d_e n_{O_2}$
 1078 is the amount of O₂ added externally to the system. At steady state, by definition $dn_{O_2} = 0$, hence $d_r n_{O_2}$
 1079 $= -d_e n_{O_2}$. Note that in this context 'external', e, refers to the system, whereas in Figure 1 'external',
 1080 ext, refers to the organism.
 1081 9 J_{V,O_2} is an experimental variable, expressed per volume of the instrument chamber.
 1082 10 $I_{O_2/NX}$ is a physiological variable, depending on the size of entity X.
 1083 11 There are many ways to normalize for a mitochondrial marker, that are used in different experimental
 1084 approaches: (1) $J_{O_2/mtE} = J_{V,O_2} \cdot C_{mtE}^{-1}$; (2) $J_{O_2/mtE} = J_{V,O_2} \cdot C_{mX}^{-1} \cdot D_{mtE}^{-1} = J_{O_2/mX} \cdot D_{mtE}^{-1}$; (3) $J_{O_2/mtE} =$
 1085 $J_{V,O_2} \cdot C_{NX}^{-1} \cdot mtE_{NX}^{-1} = I_{O_2/NX} \cdot mtE_{NX}^{-1}$; (4) $J_{O_2/mtE} = I_{O_2} \cdot mtE^{-1}$. The mt-elementary unit [mtEU] varies depending
 1086 on the mt-marker.
 1087
 1088
 1089

Table 5. Sample types, X, abbreviations, and quantification.

Identity of sample	X	N _X	Mass ^a	Volume	mt-Marker
mitochondrial preparation		[x]	[kg]	[m ³]	[mtEU]
isolated mitochondria	imt		m_{mt}	V_{mt}	mtE
tissue homogenate	thom		m_{thom}		mtE_{thom}
permeabilized tissue	pti		m_{pti}		mtE_{pti}
permeabilized fibre	pfi		m_{pfi}		mtE_{pfi}
permeabilized cell	pce	N_{pce}	M_{pce}	V_{pce}	mtE_{pce}
cells ^b	ce	N_{ce}	M_{ce}	V_{ce}	mtE_{ce}
intact cell, viable cell	vce	N_{vce}	M_{vce}	V_{vce}	
dead cell	dce	N_{dce}	M_{dce}	V_{dce}	
organism	org	N_{org}	M_{org}	V_{org}	

^a Instead of mass, the wet weight or dry weight is frequently stated, W_w or W_d . m_X is mass of the sample [kg], M_X is mass of the object [kg·x⁻¹] (Table 4).

^b Total cell count, $N_{ce} = N_{vce} + N_{dce}$

4.1. Flow: per object

4.1.1. Number concentration, C_{NX} : Normalization per sample concentration is routinely required to report respiratory data. C_{NX} is the experimental number concentration of sample X. In the case of animals, e.g., nematodes, $C_{NX} = N_X \cdot V^{-1}$ [x·L⁻¹], where N_X is the number of organisms in the chamber. Similarly, the number of cells per chamber volume is the number concentration of permeabilized or intact cells $C_{Nce} = N_{ce} \cdot V^{-1}$ [x·L⁻¹], where N_{ce} is the number of cells in the chamber (Table 4).

4.1.2. Flow per object, $I_{O_2/NX}$: O₂ flow per cell is calculated from volume-specific O₂ flux, J_{V,O_2} [nmol·s⁻¹·L⁻¹] (per V of the measurement chamber [L]), divided by the number concentration of cells. The total cell count is the sum of viable and dead cells, $N_{ce} = N_{vce} + N_{dce}$ (Table 5). The cell viability index, $VI = N_{vce} \cdot N_{ce}^{-1}$, is the ratio of viable cells (N_{vce} ; before experimental permeabilization) per total cell count. After experimental permeabilization, all cells are permeabilized, $N_{pce} = N_{ce}$. The cell viability index can be used to normalize respiration for the number of cells that have been viable before experimental permeabilization, $I_{O_2/Nvce} = I_{O_2/Nce} \cdot VI^{-1}$, considering that mitochondrial respiratory dysfunction in dead cells should be eliminated as a confounding factor.

The complexity changes when the object is a whole organism studied as an experimental model. The scaling law in respiratory physiology reveals a strong interaction between O₂ flow and individual body mass: *basal* metabolic rate (flow) does not increase linearly with body mass, whereas *maximum* mass-specific O₂ flux, \dot{V}_{O_2max} or \dot{V}_{O_2peak} , is approximately constant across a large range of individual body mass (Weibel and Hoppeler 2005). Individuals, breeds and species, however, deviate substantially

1114 from this relationship. $\dot{V}_{O_2\text{peak}}$ of human endurance athletes is 60 to 80 mL $O_2 \cdot \text{min}^{-1} \cdot \text{kg}^{-1}$ body mass,
 1115 converted to $J_{O_2\text{peak}/M_{\text{Org}}}$ of 45 to 60 $\text{nmol} \cdot \text{s}^{-1} \cdot \text{g}^{-1}$ (Gnaiger 2014; **Table 6**).

1116 4.2. Size-specific flux: per sample size

1117
 1118 **4.2.1. Sample concentration, C_{mX} :** Considering permeabilized tissue, homogenate or cells as the
 1119 sample, X , the sample mass is m_X [mg], which is frequently measured as wet or dry weight, W_w or W_d
 1120 [mg], respectively, or as amount of protein, m_{Protein} . The sample concentration is the mass of the
 1121 subsample per volume of the measurement chamber, $C_{mX} = m_X \cdot V^{-1}$ [$\text{g} \cdot \text{L}^{-1} = \text{mg} \cdot \text{mL}^{-1}$]. X is the type of
 1122 sample—isolated mitochondria, tissue homogenate, permeabilized fibres or cells (**Table 5**).

1123 **4.2.2. Size-specific flux:** Cellular O_2 flow can be compared between cells of identical size. To
 1124 take into account changes and differences in cell size, normalization is required to obtain cell size-
 1125 specific or mitochondrial marker-specific O_2 flux (Renner *et al.* 2003).

- 1126 • **Mass-specific flux, $J_{O_2/mX}$ [$\text{mol} \cdot \text{s}^{-1} \cdot \text{kg}^{-1}$]:** Mass-specific flux is obtained by expressing
 1127 respiration per mass of sample, m_X [mg]. Flow per cell is divided by mass per cell, $J_{O_2/mce} =$
 1128 $I_{O_2/Nce} \cdot M_{Nce}^{-1}$. Or chamber volume-specific flux, J_{V,O_2} , is divided by mass concentration of X in
 1129 the chamber, $J_{O_2/mX} = J_{V,O_2} \cdot C_{mX}^{-1}$.
- 1130 • **Cell volume-specific flux, $J_{O_2/VX}$ [$\text{mol} \cdot \text{s}^{-1} \cdot \text{m}^{-3}$]:** Sample volume-specific flux is obtained by
 1131 expressing respiration per volume of sample. For example, in the case of using cells as sample
 1132 will be the volume of cells added to the chamber (**Figure 6**).

1133 If size-specific O_2 flux is constant and independent of sample size, then there is no interaction
 1134 between the subsystems. For example, a 1.5 mg and a 3.0 mg muscle sample respire at identical mass-
 1135 specific flux. Mass-specific O_2 flux, however, may change with the mass of a tissue sample, cells or
 1136 isolated mitochondria in the measuring chamber, in which the nature of the interaction becomes an issue.
 1137 Therefore, cell density must be optimized, particularly in experiments carried out in wells, considering
 1138 the confluency of the cell monolayer or clumps of cells (Salabei *et al.* 2014).

1139 1140 4.3. Marker-specific flux: per mitochondrial content

1141
 1142 Tissues can contain multiple cell populations that may have distinct mitochondrial subtypes.
 1143 Mitochondria undergo dynamic fission and fusion cycles, and can exist in multiple stages and sizes that
 1144 may be altered by a range of factors. The isolation of mitochondria (often achieved through differential
 1145 centrifugation) can therefore yield a subsample of the mitochondrial types present in a tissue, depending
 1146 on the isolation protocols utilized, *e.g.*, centrifugation speed. This possible bias should be taken into
 1147 account when planning experiments using isolated mitochondria. Different sizes of mitochondria are
 1148 enriched at specific centrifugation speeds, which can be used strategically for isolation of mitochondrial
 1149 subpopulations.

1150 Part of the mitochondrial content of a tissue is lost during preparation of isolated mitochondria.
 1151 The fraction of isolated mitochondria obtained from a tissue sample is expressed as mitochondrial
 1152 recovery. At a high mitochondrial recovery, the fraction of isolated mitochondria is more representative
 1153 of the total mitochondrial population than in preparations characterized by low recovery. Determination
 1154 of the mitochondrial recovery and yield is based on measurement of the concentration of a mitochondrial
 1155 marker in the stock of isolated mitochondria, $C_{mtE,stock}$, and crude tissue homogenate, $C_{mtE,thom}$, which
 1156 simultaneously provides information on the specific mitochondrial density in the sample, D_{mtE} (**Table**
 1157 **4**).

1158 When discussing concepts of normalization, it is essential to consider the question posed by the
 1159 study. If the study aims at comparing tissue performance—such as the effects of a treatment on a specific
 1160 tissue, then normalization for tissue mass or protein content is appropriate. However, if the aim is to
 1161 find differences in mitochondrial function independent of mitochondrial density (**Table 4**), then
 1162 normalization to a mitochondrial marker is imperative (**Figure 6**). One cannot assume that quantitative
 1163 changes in various markers—such as mitochondrial proteins—necessarily occur in parallel with one
 1164 another. It should be established that the marker chosen is not selectively altered by the performed
 1165 treatment. In conclusion, the normalization must reflect the question under investigation to reach a
 1166 satisfying answer. On the other hand, the goal of comparing results across projects and institutions
 1167 requires standardization on normalization for entry into a databank.

1168 **4.3.1. Mitochondrial concentration, C_{mtE} , and mitochondrial markers:** Mitochondrial
 1169 organelles compose a dynamic cellular reticulum in various states of fusion and fission. Hence, the

1170 definition of an ‘amount’ of mitochondria is often misconceived: mitochondria cannot be counted
 1171 reliably as a number of occurring elementary components. Therefore, quantification of the amount of
 1172 mitochondria depends on the measurement of chosen mitochondrial markers. “Mitochondria are the
 1173 structural and functional elementary units of cell respiration” (Gnaiger 2014). The quantity of a
 1174 mitochondrial marker can reflect the amount of *mitochondrial elementary components*, mtE , expressed
 1175 in various mitochondrial elementary units [mtEU] specific for each measured mt-marker (**Table 4**).
 1176 However, since mitochondrial quality may change in response to stimuli—particularly in mitochondrial
 1177 dysfunction (Campos *et al.* 2017) and after exercise training (Pesta *et al.* 2011) and during aging (Daum
 1178 *et al.* 2013)—some markers can vary while others are unchanged: (1) Mitochondrial volume and
 1179 membrane area are structural markers, whereas mitochondrial protein mass is commonly used as a
 1180 marker for isolated mitochondria. (2) Molecular and enzymatic mitochondrial markers (amounts or
 1181 activities) can be selected as matrix markers, *e.g.*, citrate synthase activity, mtDNA; mtIM-markers, *e.g.*,
 1182 cytochrome *c* oxidase activity, aa_3 content, cardiolipin, or mtOM-markers, *e.g.*, the voltage-dependent
 1183 anion channel (VDAC), TOM20. (3) Extending the measurement of mitochondrial marker enzyme
 1184 activity to mitochondrial pathway capacity, ET- or OXPHOS-capacity can be considered as an
 1185 integrative functional mitochondrial marker.

1186 Depending on the type of mitochondrial marker, the mitochondrial elementary component, mtE ,
 1187 is expressed in marker-specific units. Mitochondrial concentration in the measurement chamber and the
 1188 tissue of origin are quantified as (1) a quantity for normalization in functional analyses, C_{mtE} , and (2) a
 1189 physiological output that is the result of mitochondrial biogenesis and degradation, D_{mtE} , respectively
 1190 (**Table 4**). It is recommended, therefore, to distinguish *experimental mitochondrial concentration*, C_{mtE}
 1191 $= mtE \cdot V^{-1}$ and *physiological mitochondrial density*, $D_{mtE} = mtE \cdot m_X^{-1}$. Then mitochondrial density is the
 1192 amount of mitochondrial elementary components per mass of tissue, which is a biological variable
 1193 (**Figure 6**). The experimental variable is mitochondrial density multiplied by sample mass concentration
 1194 in the measuring chamber, $C_{mtE} = D_{mtE} \cdot C_{mX}$, or mitochondrial content multiplied by sample number
 1195 concentration, $C_{mtE} = mtE_X \cdot C_{NX}$ (**Table 4**).

1196 **4.3.2. mt-Marker-specific flux, $J_{O_2/mtE}$:** Volume-specific metabolic O_2 flux depends on: (1) the
 1197 sample concentration in the volume of the instrument chamber, C_{mX} , or C_{NX} ; (2) the mitochondrial
 1198 density in the sample, $D_{mtE} = mtE \cdot m_X^{-1}$ or $mtE_X = mtE \cdot N_X^{-1}$; and (3) the specific mitochondrial activity or
 1199 performance per elementary mitochondrial unit, $J_{O_2/mtE} = J_{V,O_2} \cdot C_{mtE}^{-1}$ [$\text{mol} \cdot \text{s}^{-1} \cdot \text{mtEU}^{-1}$] (**Table 4**).
 1200 Obviously, the numerical results for $J_{O_2/mtE}$ vary with the type of mitochondrial marker chosen for
 1201 measurement of mtE and $C_{mtE} = mtE \cdot V^{-1}$ [$\text{mtEU} \cdot \text{m}^{-3}$].

1202 Different methods are involved in the quantification of mitochondrial markers and have different
 1203 strengths. Some problems are common for all mitochondrial markers, mtE : (1) Accuracy of
 1204 measurement is crucial, since even a highly accurate and reproducible measurement of O_2 flux results
 1205 in an inaccurate and noisy expression if normalized by a biased and noisy measurement of a
 1206 mitochondrial marker. This problem is acute in mitochondrial respiration because the denominators used
 1207 (the mitochondrial markers) are often small moieties of which accurate and precise determination is
 1208 difficult. This problem can be avoided when O_2 fluxes measured in substrate-uncoupler-inhibitor
 1209 titration protocols are normalized for flux in a defined respiratory reference state, which is used as an
 1210 *internal* marker and yields flux control ratios, $FCRs$. $FCRs$ are independent of externally measured
 1211 markers and, therefore, are statistically robust, considering the limitations of ratios in general (Jasienski
 1212 and Bazzaz 1999). $FCRs$ indicate qualitative changes of mitochondrial respiratory control, with highest
 1213 quantitative resolution, separating the effect of mitochondrial density or concentration on $J_{O_2/mX}$ and
 1214 $J_{O_2/NX}$ from that of function per elementary mitochondrial marker, $J_{O_2/mtE}$ (Pesta *et al.* 2011; Gnaiger
 1215 2014). (2) If mitochondrial quality does not change and only the amount of mitochondria varies as a
 1216 determinant of mass-specific flux, any marker is equally qualified in principle; then in practice selection
 1217 of the optimum marker depends only on the accuracy and precision of measurement of the mitochondrial
 1218 marker. (3) If mitochondrial flux control ratios change, then there may not be any best mitochondrial
 1219 marker. In general, measurement of multiple mitochondrial markers enables a comparison and
 1220 evaluation of normalization for these mitochondrial markers. Particularly during postnatal development,
 1221 the activity of marker enzymes—such as cytochrome *c* oxidase and citrate synthase—follows different
 1222 time courses (Drahota *et al.* 2004). Evaluation of mitochondrial markers in healthy controls is
 1223 insufficient for providing guidelines for application in the diagnosis of pathological states and specific
 1224 treatments.

In line with the concept of the respiratory control ratio (Chance and Williams 1955a), the most readily used normalization is that of flux control ratios and flux control factors (Gnaiger 2014). Selection of the state of maximum flux in a protocol as the reference state has the advantages of: (1) internal normalization; (2) statistically validated linearization of the response in the range of 0 to 1; and (3) consideration of maximum flux for integrating a large number of elementary steps in the OXPHOS- or ET-pathways. This reduces the risk of selecting a functional marker that is specifically altered by the treatment or pathology, yet increases the chance that the highly integrative pathway is disproportionately affected, *e.g.*, the OXPHOS- rather than ET-pathway in case of an enzymatic defect in the phosphorylation-pathway. In this case, additional information can be obtained by reporting flux control ratios based on a reference state that indicates stable tissue-mass specific flux.

Stereological measurement of mitochondrial content via two-dimensional transmission electron microscopy is considered as the gold standard in determination of mitochondrial volume fractions in cells and tissues (Weibel, Hoppeler, 2005). Accurate determination of three-dimensional volume by two-dimensional microscopy, however, is both time consuming and statistically challenging (Larsen *et al.* 2012). The validity of using mitochondrial marker enzymes (citrate synthase activity, CI to CIV amount or activity) for normalization of flux is limited in part by the same factors that apply to flux control ratios. Strong correlations between various mitochondrial markers and citrate synthase activity (Reichmann *et al.* 1985; Boushel *et al.* 2007; Mogensen *et al.* 2007) are expected in a specific tissue of healthy persons and in disease states not specifically targeting citrate synthase. Citrate synthase activity is acutely modifiable by exercise (Tonkonogi *et al.* 1997; Leek *et al.* 2001). Evaluation of mitochondrial markers related to a selected age and sex cohort cannot be extrapolated to provide recommendations for normalization in respirometric diagnosis of disease, in different states of development and ageing, different cell types, tissues, and species. mtDNA normalized to nDNA via qPCR is correlated to functional mitochondrial markers including OXPHOS- and ET-capacity in some cases (Puntschart *et al.* 1995; Wang *et al.* 1999; Menshikova *et al.* 2006; Boushel *et al.* 2007; Ehinger *et al.* 2015), but lack of such correlations have been reported (Menshikova *et al.* 2005; Schultz and Wiesner 2000; Pesta *et al.* 2011). Several studies indicate a strong correlation between cardiolipin content and increase in mitochondrial function with exercise (Menshikova *et al.* 2005; Menshikova *et al.* 2007; Larsen *et al.* 2012; Faber *et al.* 2014), but it has not been evaluated as a general mitochondrial biomarker in disease. With no single best mitochondrial marker, a good strategy is to quantify several different biomarkers to minimize the decorrelating effects caused by diseases, treatments, or other factors. Determination of multiple markers, particularly a matrix marker and a marker from the mtIM, allows tracking changes in mitochondrial quality defined by their ratio.

5. Normalization of rate per system

5.1. Flow: per chamber

The experimental system (experimental chamber) is part of the measurement instrument, separated from the environment as an isolated, closed, open, isothermal or non-isothermal system (Table 4). Reporting O₂ flows per respiratory chamber, I_{O_2} [nmol·s⁻¹], restricts the analysis to intra-experimental comparison of relative differences.

5.2. Flux: per chamber volume

5.2.1. System-specific flux, J_{V,O_2} : We distinguish between (1) the *system* with volume V and mass m defined by the system boundaries, and (2) the *sample* or *objects* with volume V_X and mass m_X that are enclosed in the experimental chamber (Figure 6). Metabolic O₂ flow per object, I_{O_2/N_X} , is the total O₂ flow in the system divided by the number of objects, N_X , in the system. I_{O_2/N_X} increases as the mass of the object is increased. Sample mass-specific O₂ flux, J_{O_2/m_X} should be independent of the mass of the sample studied in the instrument chamber, but system volume-specific O₂ flux, J_{V,O_2} (per volume of the instrument chamber), increases in proportion to the mass of the sample in the chamber. Although J_{V,O_2} depends on mass-concentration of the sample in the chamber, it should be independent of the chamber (system) volume at constant sample mass-concentration. There are practical limitations to increasing the

1280 mass-concentration of the sample in the chamber, when one is concerned about crowding effects and
 1281 instrumental time resolution.

1282 **5.2.2. Advancement per volume:** When the reactor volume does not change during the reaction,
 1283 which is typical for liquid phase reactions, the volume-specific *flux of a chemical reaction* r is the time
 1284 derivative of the advancement of the reaction per unit volume, $J_{V,rB} = d_r \xi_B / dt \cdot V^{-1}$ [(mol·s⁻¹)·L⁻¹]. The *rate*
 1285 *of concentration change* is dc_B/dt [(mol·L⁻¹)·s⁻¹], where concentration is $c_B = n_B \cdot V^{-1}$. There is a difference
 1286 between (1) J_{V,rO_2} [mol·s⁻¹·L⁻¹] and (2) rate of concentration change [mol·L⁻¹·s⁻¹]. These merge into a
 1287 single expression only in closed systems. In open systems, internal transformations (catabolic flux, O₂
 1288 consumption) are distinguished from external flux (such as O₂ supply). External fluxes of all substances
 1289 are zero in closed systems. In a closed chamber O₂ consumption (internal flux of catabolic reactions k ;
 1290 I_{kO_2} [pmol·s⁻¹]) causes a decline in the amount of O₂ in the system, n_{O_2} [nmol]. Normalization of these
 1291 quantities for the volume of the system, V [L \equiv dm³], yields volume-specific O₂ flux, $J_{V,kO_2} = I_{kO_2}/V$
 1292 [nmol·s⁻¹·L⁻¹], and O₂ concentration, [O₂] or $c_{O_2} = n_{O_2} \cdot V^{-1}$ [μ mol·L⁻¹ = μ M = nmol·mL⁻¹]. Instrumental
 1293 background O₂ flux is due to external flux into a non-ideal closed respirometer, so total volume-specific
 1294 flux has to be corrected for instrumental background O₂ flux—O₂ diffusion into or out of the
 1295 instrumental chamber. J_{V,kO_2} is relevant mainly for methodological reasons and should be compared with
 1296 the accuracy of instrumental resolution of background-corrected flux, *e.g.*, ± 1 nmol·s⁻¹·L⁻¹ (Gnaiger
 1297 2001). ‘Catabolic’ indicates O₂ flux, J_{kO_2} , corrected for: (1) instrumental background O₂ flux; (2)
 1298 chemical background O₂ flux due to autoxidation of chemical components added to the incubation
 1299 medium; and (3) *Rox* for O₂-consuming side reactions unrelated to the catabolic pathway k .

1300
 1301

1302 6. Conversion of units

1303

1304 Many different units have been used to report the O₂ consumption rate, OCR (**Table 6**). SI base
 1305 units provide the common reference to introduce the theoretical principles (**Figure 6**), and are used with
 1306 appropriately chosen SI prefixes to express numerical data in the most practical format, with an effort
 1307 towards unification within specific areas of application (**Table 7**). Reporting data in SI units—including
 1308 the mole [mol], coulomb [C], joule [J], and second [s]—should be encouraged, particularly by journals
 1309 that propose the use of SI units.

1310

1311 **Table 6. Conversion of various formats and units used in respirometry and**
 1312 **ergometry.** e^- is the number of electrons or reducing equivalents. z_B is the charge number
 1313 of entity B.

1314

Format	1 Unit		Multiplication factor	SI-unit	Notes
\underline{n}	ng.atom O·s ⁻¹	(2 e^-)	0.5	nmol O ₂ ·s ⁻¹	
\underline{n}	ng.atom O·min ⁻¹	(2 e^-)	8.33	pmol O ₂ ·s ⁻¹	
\underline{n}	natom O·min ⁻¹	(2 e^-)	8.33	pmol O ₂ ·s ⁻¹	
\underline{n}	nmol O ₂ ·min ⁻¹	(4 e^-)	16.67	pmol O ₂ ·s ⁻¹	
\underline{n}	nmol O ₂ ·h ⁻¹	(4 e^-)	0.2778	pmol O ₂ ·s ⁻¹	
\underline{V} to \underline{n}	mL O ₂ ·min ⁻¹ at STPD ^a		0.744	μ mol O ₂ ·s ⁻¹	1
\underline{e} to \underline{n}	$W = J/s$ at -470 kJ/mol O ₂		-2.128	μ mol O ₂ ·s ⁻¹	
\underline{e} to \underline{n}	mA = mC·s ⁻¹	($z_{H^+} = 1$)	10.36	nmol H ⁺ ·s ⁻¹	2
\underline{e} to \underline{n}	mA = mC·s ⁻¹	($z_{O_2} = 4$)	2.59	nmol O ₂ ·s ⁻¹	2
\underline{n} to \underline{e}	nmol H ⁺ ·s ⁻¹	($z_{H^+} = 1$)	0.09649	mA	3
\underline{n} to \underline{e}	nmol O ₂ ·s ⁻¹	($z_{O_2} = 4$)	0.38594	mA	3

1315 1 At standard temperature and pressure dry (STPD: 0 °C = 273.15 K and 1 atm = 101.325 kPa =
 1316 760 mmHg), the molar volume of an ideal gas, V_m , and V_{m,O_2} is 22.414 and 22.392 L·mol⁻¹,
 1317 respectively. Rounded to three decimal places, both values yield the conversion factor of 0.744.

- 1318 For comparison at normal temperature and pressure dry (NTPD: 20 °C), V_{m,O_2} is 24.038 L·mol⁻¹.
 1319 Note that the SI standard pressure is 100 kPa.
 1320 2 The multiplication factor is $10^6/(z_B \cdot F)$.
 1321 3 The multiplication factor is $z_B \cdot F/10^6$.

1322
 1323

Table 7. Conversion of units with preservation of numerical values.

Name	Frequently used unit	Equivalent unit	Notes
volume-specific flux, J_{V,O_2}	pmol·s ⁻¹ ·mL ⁻¹	nmol·s ⁻¹ ·L ⁻¹	1
	mmol·s ⁻¹ ·L ⁻¹	mol·s ⁻¹ ·m ⁻³	
cell-specific flow, $I_{O_2/cell}$	pmol·s ⁻¹ ·10 ⁻⁶ cells	amol·s ⁻¹ ·cell ⁻¹	2
	pmol·s ⁻¹ ·10 ⁻⁹ cells	zmol·s ⁻¹ ·cell ⁻¹	3
cell number concentration, C_{Nce}	10 ⁶ cells·mL ⁻¹	10 ⁹ cells·L ⁻¹	
mitochondrial protein concentration, C_{mtE}	0.1 mg·mL ⁻¹	0.1 g·L ⁻¹	
mass-specific flux, $J_{O_2/m}$	pmol·s ⁻¹ ·mg ⁻¹	nmol·s ⁻¹ ·g ⁻¹	4
catabolic power, P_k	μW·10 ⁻⁶ cells	pW·cell ⁻¹	1
volume	1,000 L	m ³ (1,000 kg)	
	L	dm ³ (kg)	
	mL	cm ³ (g)	
	μL	mm ³ (mg)	
	fL	μm ³ (pg)	5
amount of substance concentration	M = mol·L ⁻¹	mol·dm ⁻³	

- 1324 1 pmol: picomole = 10⁻¹² mol
 1325 2 amol: attomole = 10⁻¹⁸ mol
 1326 3 zmol: zeptomole = 10⁻²¹ mol

1327

1328 Although volume is expressed as m³ using the SI base unit, the litre [dm³] is a conventional unit
 1329 of volume for concentration and is used for most solution chemical kinetics. If one multiplies $I_{O_2/Nce}$ by
 1330 C_{Nce} , then the result will not only be the amount of O₂ [mol] consumed per time [s⁻¹] in one litre [L⁻¹],
 1331 but also the change in O₂ concentration per second (for any volume of an ideally closed system). This
 1332 is ideal for kinetic modeling as it blends with chemical rate equations where concentrations are typically
 1333 expressed in mol·L⁻¹ (Wagner *et al.* 2011). In studies of multinuclear cells—such as differentiated
 1334 skeletal muscle cells—it is easy to determine the number of nuclei but not the total number of cells. A
 1335 generalized concept, therefore, is obtained by substituting cells by nuclei as the sample entity. This does
 1336 not hold, however, for non-nucleated platelets.

1337 For studies of cells, we recommend that respiration be expressed, as far as possible, as: (1) O₂
 1338 flux normalized for a mitochondrial marker, for separation of the effects of mitochondrial quality and
 1339 content on cell respiration (this includes $FCRs$ as a normalization for a functional mitochondrial
 1340 marker); (2) O₂ flux in units of cell volume or mass, for comparison of respiration of cells with different
 1341 cell size (Renner *et al.* 2003) and with studies on tissue preparations, and (3) O₂ flow in units of attomole
 1342 (10⁻¹⁸ mol) of O₂ consumed per second by each cell [amol·s⁻¹·cell⁻¹], numerically equivalent to
 1343 [pmol·s⁻¹·10⁻⁶ cells]. This convention allows information to be easily used when designing experiments
 1344 in which O₂ flow must be considered. For example, to estimate the volume-specific O₂ flux in an
 1345 instrument chamber that would be expected at a particular cell number concentration, one simply needs
 1346 to multiply the flow per cell by the number of cells per volume of interest. This provides the amount of
 1347 O₂ [mol] consumed per time [s⁻¹] per unit volume [L⁻¹]. At an O₂ flow of 100 amol·s⁻¹·cell⁻¹ and a cell
 1348 density of 10⁹ cells·L⁻¹ (10⁶ cells·mL⁻¹), the volume-specific O₂ flux is 100 nmol·s⁻¹·L⁻¹ (100
 1349 pmol·s⁻¹·mL⁻¹).

1350 ET-capacity in human cell types including HEK 293, primary HUVEC, and fibroblasts ranges
 1351 from 50 to 180 amol·s⁻¹·cell⁻¹, measured in intact cells in the noncoupled state (see Gnaiger 2014). At
 1352 100 amol·s⁻¹·cell⁻¹ corrected for R_{ox} , the current across the mt-membranes, I_{H+e} , approximates 193
 1353 pA·cell⁻¹ or 0.2 nA per cell. See Rich (2003) for an extension of quantitative bioenergetics from the

1354 molecular to the human scale, with a transmembrane proton flux equivalent to 520 A in an adult at a
 1355 catabolic power of -110 W. Modelling approaches illustrate the link between protonmotive force and
 1356 currents (Willis *et al.* 2016).

1357 We consider isolated mitochondria as powerhouses and proton pumps as molecular machines to
 1358 relate experimental results to energy metabolism of the intact cell. The cellular P_{\gg}/O_2 based on oxidation
 1359 of glycogen is increased by the glycolytic (fermentative) substrate-level phosphorylation of 3 $P_{\gg}/Glyc$
 1360 or 0.5 mol P_{\gg} for each mol O_2 consumed in the complete oxidation of a mol glycosyl unit (Glyc). Adding
 1361 0.5 to the mitochondrial P_{\gg}/O_2 ratio of 5.4 yields a bioenergetic cell physiological P_{\gg}/O_2 ratio close to
 1362 6. Two NADH equivalents are formed during glycolysis and transported from the cytosol into the
 1363 mitochondrial matrix, either by the malate-aspartate shuttle or by the glycerophosphate shuttle (**Figure**
 1364 **2A**) resulting in different theoretical yields of ATP generated by mitochondria, the energetic cost of
 1365 which potentially must be taken into account. Considering also substrate-level phosphorylation in the
 1366 TCA cycle, this high P_{\gg}/O_2 ratio not only reflects proton translocation and OXPHOS studied in isolation,
 1367 but integrates mitochondrial physiology with energy transformation in the living cell (Gnaiger 1993a).
 1368
 1369

1370 7. Conclusions

1371
 1372 Catabolic cell respiration is the process of exergonic and exothermic energy transformation in
 1373 which scalar redox reactions are coupled to vectorial ion translocation across a semipermeable
 1374 membrane, which separates the small volume of a bacterial cell or mitochondrion from the larger volume
 1375 of its surroundings. The electrochemical exergy can be partially conserved in the phosphorylation of
 1376 ADP to ATP or in ion pumping, or dissipated in an electrochemical short-circuit. Respiration is thus
 1377 clearly distinguished from fermentation as the counterparts of cellular core energy metabolism. An O_2
 1378 flux balance scheme illustrates the relationships and general definitions (**Figures 1 and 2**).
 1379

1380 **Box 3: Recommendations for studies with mitochondrial preparations**

- 1381 • Normalization of respiratory rates should be provided as far as possible:
 - 1382 1. *Biophysical normalization*: on a per cell basis as O_2 flow; this may not be possible when
 - 1383 dealing with coenocytic organisms, *e.g.*, filamentous fungi, or tissues without cross-
 - 1384 walls separating individual cells, *e.g.*, muscle fibers.
 - 1385 2. *Cellular normalization*: per g protein; per cell- or tissue-mass as mass-specific O_2 flux;
 - 1386 per cell volume as cell volume-specific flux.
 - 1387 3. *Mitochondrial normalization*: per mitochondrial marker as mt-specific flux.
- 1388 With information on cell size and the use of multiple normalizations, maximum potential information
 1389 is available (Renner *et al.* 2003; Wagner *et al.* 2011; Gnaiger 2014). Reporting flow in a respiratory
 1390 chamber [$nmol \cdot s^{-1}$] is discouraged, since it restricts the analysis to intra-experimental comparison of
 1391 relative (qualitative) differences.
- 1392 • Catabolic mitochondrial respiration is distinguished from residual O_2 consumption. Fluxes in
 1393 mitochondrial coupling states should be, as far as possible, corrected for residual O_2 consumption.
- 1394 • Different mechanisms of uncoupling should be distinguished by defined terms. The tightness of
 1395 coupling relates to these uncoupling mechanisms, whereas the coupling stoichiometry varies as a
 1396 function the substrate type involved in ET-pathways with either three or two redox proton pumps
 1397 operating in series. Separation of tightness of coupling from the pathway-dependent coupling
 1398 stoichiometry is possible only when the substrate type undergoing oxidation remains the same for
 1399 respiration in LEAK-, OXPHOS-, and ET-states. In studies of the tightness of coupling, therefore,
 1400 simple substrate-inhibitor combinations should be applied to exclude a shift in substrate competition
 1401 that may occur when providing physiological substrate cocktails.
- 1402 • In studies of isolated mitochondria, the mitochondrial recovery and yield should be reported.
 1403 Experimental criteria such as transmission electron microscopy for evaluation of purity versus
 1404 integrity should be considered. Mitochondrial markers—such as citrate synthase activity as an
 1405 enzymatic matrix marker—provide a link to the tissue of origin on the basis of calculating the
 1406 mitochondrial recovery, *i.e.*, the fraction of mitochondrial marker obtained from a unit mass of tissue.
 1407 Total mitochondrial protein is frequently applied as a mitochondrial marker, which is restricted to
 1408 isolated mitochondria.
 1409

- 1410 • In studies of permeabilized cells, the viability of the cell culture or cell suspension of origin should
 1411 be reported. Normalization should be evaluated for total cell count or viable cell count.
 1412 • Terms and symbols are summarized in **Table 8**. Their use will facilitate transdisciplinary
 1413 communication and support further development of a consistent theory of bioenergetics and
 1414 mitochondrial physiology. Technical terms related to and defined with normal words can be used as
 1415 index terms in databases, support the creation of ontologies towards semantic information processing
 1416 (MitoPedia), and help in communicating analytical findings as impactful data-driven stories.
 1417 ‘Making data available without making it understandable may be worse than not making it available
 1418 at all’ (National Academies of Sciences, Engineering, and Medicine 2018). Success will depend on
 1419 taking further steps: (1) exhaustive text-mining considering Omics data and functional data; (2)
 1420 network analysis of Omics data with bioinformatics tools; (3) cross-validation with distinct
 1421 bioinformatics approaches; (4) correlation with functional data; (5) guidelines for biological
 1422 validation of network data. This is a call to carefully contribute to FAIR principles (Findable,
 1423 Accessible, Interoperable, Reusable) for the sharing of scientific data.
 1424

1425
 1426 **Table 8. Terms, symbols, and units.**
 1427
 1428

1429 1430	Term	Symbol	Unit	Links and comments
1431	alternative quinol oxidase	AOX		Figure 2B
1432	adenosine monophosphate	AMP		2 ADP ↔ ATP+AMP
1433	adenosine diphosphate	ADP		Table 1; Figures 1, 2 and 5
1434	adenosine triphosphate	ATP		Figures 2 and 5
1435	adenylates	AMP, ADP, ATP		Section 2.5.1
1436	amount of substance B	n_B	[mol]	
1437	ATP yield per O ₂	Y_{P/O_2}		P _» /O ₂ ratio measured in any respiratory state
1438	catabolic reaction	k		Figures 1 and 3
1439	catabolic respiration	J_{kO_2}	<i>varies</i>	Figures 1 and 3
1440	cell respiration	J_{rO_2}	<i>varies</i>	Figure 1
1441	cell viability index	VI		$VI = N_{vce} \cdot N_{ce}^{-1} = 1 - N_{dce} \cdot N_{ce}^{-1}$
1442	charge number of entity B	z_B		Table 6; $z_{O_2} = 4$
1443	Complexes I to IV	CI to CIV		respiratory ET Complexes; Figure 2B
1444	concentration of substance B	$c_B = n_B \cdot V^{-1}$; [B]	[mol·m ⁻³]	Box 2
1445	coupling control state	CCS		Section 2.4.1
1446	dead cell number	N_{dce}	[x]	non-viable cells, loss of plasma membrane barrier function; Table 5
1447	electric format	e	[C]	Table 6
1448	electron transfer system	ETS		state; Figures 2B and 4
1449	ET state	ET		Table 1; Figures 2B and 4; State 3u
1450	ET-capacity	E	<i>varies</i>	Table 1; Figure 4
1451	flow, for substance B	I_B	[mol·s ⁻¹]	system-related extensive quantity; Figure 6
1452	flux, for substance B	J_B	<i>varies</i>	size-specific quantity; Figure 6
1453	inorganic phosphate	P _i		Figure 2C
1454	inorganic phosphate carrier	PiC		Figure 2C
1455	intact cell number, viable cell number	N_{vce}	[x]	viable cells, intact plasma membrane barrier function; Table 5
1456	LEAK state	LEAK		state; Table 1; Figure 4; compare State 4
1457	LEAK-respiration	L	<i>varies</i>	Table 1; Figure 4
1458	mass format	m	[kg]	Table 4; Figure 6
1459	mass of sample X	m_X	[kg]	Table 4

1468	mass, dry mass	m_d	[kg]	mass of sample X ; Figure 6 (frequently called dry weight)
1469				
1470	mass, wet mass	m_w	[kg]	mass of sample X ; Figure 6 (frequently called wet weight)
1471				
1472	mass of object X	$M_X = m_X \cdot N_X^{-1}$	[kg·x ⁻¹]	mass of entity X ; Table 4
1473	MITOCARTA			https://www.broadinstitute.org/scientific-community/science/programs/metabolic-disease-program/publications/mitocarta/mitocarta-in-0
1474				
1475				
1476				
1477				
1478	MitoPedia			http://www.bioblast.at/index.php/MitoPedia
1479	mitochondria or mitochondrial	mt		Box 1
1480	mitochondrial DNA	mtDNA		Box 1
1481	mitochondrial concentration	$C_{mtE} = mtE \cdot V^{-1}$	[mtEU·m ⁻³]	Table 4
1482	mitochondrial content	mtE_X	[mtEU·x ⁻¹]	$mtE_X = mtE \cdot N_X^{-1}$; Table 4
1483	mitochondrial			
1484	elementary component	mtE	[mtEU]	quantity of mt-marker; Table 4
1485	mitochondrial elementary unit	mtEU	<i>varies</i>	specific units for mt-marker; Table 4
1486	mitochondrial inner membrane	mtIM		MIM is widely used; the first M is replaced by mt; Figure 2; Box 1
1487				
1488	mitochondrial outer membrane	mtOM		MOM is widely used; the first M is replaced by mt; Figure 2; Box 1
1489				
1490	mitochondrial recovery	Y_{mtE}		fraction of mtE recovered in sample from the tissue of origin
1491				
1492	mitochondrial yield	$Y_{mtE/m}$		mt-yield per tissues mass; $Y_{mtE/m} = Y_{mtE} \cdot D_{mtE}$
1493				
1494	molar format	\underline{n}	[mol]	Table 6
1495	negative	neg		Figure 4
1496	number concentration of X	C_{NX}	[x·m ⁻³]	Table 4
1497	number format	\underline{N}	[x]	Table 4; Figure 6
1498	number of cells	N_{ce}	[x]	$N_{ce} = N_{vce} + N_{dce}$; Table 5
1499	number of entities X	N_X	[x]	Table 4; Figure 6
1500	number of entity B	N_B	[x]	Table 4
1501	oxidative phosphorylation	OXPPOS		state; Table 1; Figure 4
1502	OXPPOS state	OXPPOS		Table 1; State 3 if [ADP] and [P _i] are saturating
1503				
1504	OXPPOS-capacity	P	<i>varies</i>	Table 1; Figure 4
1505	oxygen concentration	$c_{O_2} = n_{O_2} \cdot V^{-1}$	[mol·m ⁻³]	[O ₂]; Section 3.2
1506	oxygen flux, in reaction r	J_{rO_2}	<i>varies</i>	Figure 1
1507	pathway control state	PCS		Section 2.2
1508	permeability transition	mtPT		Figure 3; Section 2.4.3; MPT is widely used; M is replaced by mt
1509				
1510	permeabilized cell number	N_{pce}	[x]	experimental permeabilization of plasma membrane; Table 5
1511				
1512	phosphorylation of ADP to ATP	$P \gg$		Section 2.2
1513	$P \gg / O_2$ ratio	$P \gg / O_2$		mechanistic $Y_{P \gg / O_2}$, calculated from pump stoichiometries; Figure 2B
1514				
1515	positive	pos		Figure 4
1516	proton in the negative compartment	H^+_{neg}		Figure 4
1517	proton in the positive compartment	H^+_{pos}		Figure 4
1518	protonmotive force	pmf	[V]	Figures 1, 2A and 4; Table 1
1519	rate of electron transfer in ET state	E	<i>varies</i>	ET-capacity; Table 1
1520	rate of LEAK-respiration	L	<i>varies</i>	Table 1: $L(n)$, $L(T)$, $L(Omy)$
1521	rate of oxidative phosphorylation	P	<i>varies</i>	OXPPOS-capacity; Table 1
1522	rate of residual oxygen consumption	Rox		Table 1; Figure 1
1523	residual oxygen consumption	ROX; Rox		state ROX; rate Rox ; Table 1

1524	respiratory supercomplex	$SC_{I_n III_n IV_n}$	supramolecular assemblies
1525			composed of variable copy numbers
1526			(n) of CI, CIII and CIV; Box 1
1527	specific mitochondrial density	$D_{mtE} = mtE \cdot m_X^{-1}$ [mtEU·kg ⁻¹]	Table 4
1528	substrate-uncoupler-inhibitor-		
1529	titration protocol	SUIT	Section 2.2
1530	volume	V	[m ⁻³] Table 7
1531	volume format	\underline{V}	[m ⁻³] Table 6
1532			

Experimentally, respiration is separated in mitochondrial preparations from the interactions with the fermentative pathways of the intact cell. OXPHOS analysis is based on the study of mitochondrial preparations complementary to bioenergetic investigations of (1) submitochondrial particles and molecular structures, (2) intact cells, and (3) organisms—from model organisms to the human species including healthy and diseased persons (patients). Different mechanisms of respiratory uncoupling have to be distinguished (**Figure 3**). Metabolic fluxes measured in defined coupling and pathway control states (**Figures 5 and 6**) provide insights into the meaning of cellular and organismic respiration.

The optimal choice for expressing mitochondrial and cell respiration as O₂ flow per biological sample, and normalization for specific tissue-markers (volume, mass, protein) and mitochondrial markers (volume, protein, content, mtDNA, activity of marker enzymes, respiratory reference state) is guided by the scientific question under study. Interpretation of the data depends critically on appropriate normalization (**Figure 6**).

MitoEAGLE can serve as a gateway to better diagnose mitochondrial respiratory adaptations and defects linked to genetic variation, age-related health risks, sex-specific mitochondrial performance, lifestyle with its effects on degenerative diseases, and thermal and chemical environment. The present recommendations on coupling control states and rates, linked to the concept of the protonmotive force, are focused on studies using mitochondrial preparations (**Box 3**). These will be extended in a series of reports on pathway control of mitochondrial respiration, respiratory states in intact cells, and harmonization of experimental procedures.

Acknowledgements

We thank Beno M for management assistance, and Rich PR for valuable discussions. This publication is based upon work from COST Action CA15203 MitoEAGLE, supported by COST (European Cooperation in Science and Technology), in cooperation with COST Actions CA16225 EU-CARDIOPROTECTION and CA17129 CardioRNA, and K-Regio project MitoFit funded by the Tyrolian Government.

Author contributions

This manuscript developed as an open invitation to scientists and students to join as coauthors in the bottom-up spirit of COST, based on a first draft written by the corresponding author, who integrated coauthor contributions in a sequence of Open Access versions. Coauthors contributed to the scope and quality of the manuscript, may have focused on a particular section, and are listed in alphabetical order. Coauthors confirm that they have read the final manuscript and agree to implement the recommendations into future manuscripts, presentations and teaching materials.

Competing financial interests: E.G. is founder and CEO of Oroboros Instruments, Innsbruck, Austria.

References

- Altmann R (1894) Die Elementarorganismen und ihre Beziehungen zu den Zellen. Zweite vermehrte Auflage. Verlag Von Veit & Comp, Leipzig:160 pp.
- Baggeto LG, Testa-Perussini R (1990) Role of acetoin on the regulation of intermediate metabolism of Ehrlich ascites tumor mitochondria: its contribution to membrane cholesterol enrichment modifying passive proton permeability. Arch Biochem Biophys 283:341-8.
- Beard DA (2005) A biophysical model of the mitochondrial respiratory system and oxidative phosphorylation. PLoS Comput Biol 1(4):e36.

- 1580 Benda C (1898) Weitere Mitteilungen über die Mitochondria. *Verh Dtsch Physiol Ges*:376-83.
- 1581 Birkedal R, Laasmaa M, Vendelin M (2014) The location of energetic compartments affects energetic
1582 communication in cardiomyocytes. *Front Physiol* 5:376.
- 1583 Blier PU, Dufresne F, Burton RS (2001) Natural selection and the evolution of mtDNA-encoded peptides:
1584 evidence for intergenomic co-adaptation. *Trends Genet* 17:400-6.
- 1585 Blier PU, Guderley HE (1993) Mitochondrial activity in rainbow trout red muscle: the effect of temperature on
1586 the ADP-dependence of ATP synthesis. *J Exp Biol* 176:145-58.
- 1587 Breton S, Beaupré HD, Stewart DT, Hoeh WR, Blier PU (2007) The unusual system of doubly uniparental
1588 inheritance of mtDNA: isn't one enough? *Trends Genet* 23:465-74.
- 1589 Brown GC (1992) Control of respiration and ATP synthesis in mammalian mitochondria and cells. *Biochem J*
1590 284:1-13.
- 1591 Burger G, Gray MW, Forget L, Lang BF (2013) Strikingly bacteria-like and gene-rich mitochondrial genomes
1592 throughout jakobid protists. *Genome Biol Evol* 5:418-38.
- 1593 Calvo SE, Klauser CR, Mootha VK (2016) MitoCarta2.0: an updated inventory of mammalian mitochondrial
1594 proteins. *Nucleic Acids Research* 44:D1251-7.
- 1595 Calvo SE, Julien O, Clauser KR, Shen H, Kamer KJ, Wells JA, Mootha VK (2017) Comparative analysis of
1596 mitochondrial N-termini from mouse, human, and yeast. *Mol Cell Proteomics* 16:512-23.
- 1597 Campos JC, Queliconi BB, Bozi LHM, Bechara LRG, Dourado PMM, Andres AM, Jannig PR, Gomes KMS,
1598 Zambelli VO, Rocha-Resende C, Guatimosim S, Brum PC, Mochly-Rosen D, Gottlieb RA, Kowaltowski AJ,
1599 Ferreira JCB (2017) Exercise reestablishes autophagic flux and mitochondrial quality control in heart failure.
1600 *Autophagy* 13:1304-317.
- 1601 Canton M, Luvisetto S, Schmehl I, Azzone GF (1995) The nature of mitochondrial respiration and discrimination
1602 between membrane and pump properties. *Biochem J* 310:477-81.
- 1603 Carrico C, Meyer JG, He W, Gibson BW, Verdin E (2018) The mitochondrial acylome emerges: proteomics,
1604 regulation by Sirtuins, and metabolic and disease implications. *Cell Metab* 27:497-512.
- 1605 Chan DC (2006) Mitochondria: dynamic organelles in disease, aging, and development. *Cell* 125:1241-52.
- 1606 Chance B, Williams GR (1955a) Respiratory enzymes in oxidative phosphorylation. I. Kinetics of oxygen
1607 utilization. *J Biol Chem* 217:383-93.
- 1608 Chance B, Williams GR (1955b) Respiratory enzymes in oxidative phosphorylation. III. The steady state. *J Biol*
1609 *Chem* 217:409-27.
- 1610 Chance B, Williams GR (1955c) Respiratory enzymes in oxidative phosphorylation. IV. The respiratory chain. *J*
1611 *Biol Chem* 217:429-38.
- 1612 Chance B, Williams GR (1956) The respiratory chain and oxidative phosphorylation. *Adv Enzymol Relat Subj*
1613 *Biochem* 17:65-134.
- 1614 Chowdhury SK, Djordjevic J, Albensi B, Fernyhough P (2015) Simultaneous evaluation of substrate-dependent
1615 oxygen consumption rates and mitochondrial membrane potential by TMRM and safranin in cortical
1616 mitochondria. *Biosci Rep* 36:e00286.
- 1617 Cobb LJ, Lee C, Xiao J, Yen K, Wong RG, Nakamura HK, Mehta HH, Gao Q, Ashur C, Huffman DM, Wan J,
1618 Muzumdar R, Barzilai N, Cohen P (2016) Naturally occurring mitochondrial-derived peptides are age-
1619 dependent regulators of apoptosis, insulin sensitivity, and inflammatory markers. *Aging (Albany NY)* 8:796-
1620 809.
- 1621 Cohen ER, Cvitas T, Frey JG, Holmström B, Kuchitsu K, Marquardt R, Mills I, Pavese F, Quack M, Stohner J,
1622 Strauss HL, Takami M, Thor HL (2008) Quantities, units and symbols in physical chemistry, IUPAC Green
1623 Book, 3rd Edition, 2nd Printing, IUPAC & RSC Publishing, Cambridge.
- 1624 Cooper H, Hedges LV, Valentine JC, eds (2009) The handbook of research synthesis and meta-analysis. Russell
1625 Sage Foundation.
- 1626 Coopersmith J (2010) Energy, the subtle concept. The discovery of Feynman's blocks from Leibnitz to Einstein.
1627 Oxford University Press:400 pp.
- 1628 Cummins J (1998) Mitochondrial DNA in mammalian reproduction. *Rev Reprod* 3:172-82.
- 1629 Dai Q, Shah AA, Garde RV, Yonish BA, Zhang L, Medvitz NA, Miller SE, Hansen EL, Dunn CN, Price TM
1630 (2013) A truncated progesterone receptor (PR-M) localizes to the mitochondrion and controls cellular
1631 respiration. *Mol Endocrinol* 27:741-53.
- 1632 Daum B, Walter A, Horst A, Osiewacz HD, Kühlbrandt W (2013) Age-dependent dissociation of ATP synthase
1633 dimers and loss of inner-membrane cristae in mitochondria. *Proc Natl Acad Sci U S A* 110:15301-6.
- 1634 Divakaruni AS, Brand MD (2011) The regulation and physiology of mitochondrial proton leak. *Physiology*
1635 (Bethesda) 26:192-205.
- 1636 Doerrier C, Garcia-Souza LF, Krumschnabel G, Wohlfarter Y, Mészáros AT, Gnaiger E (2018) High-Resolution
1637 Fluorespirometry and OXPHOS protocols for human cells, permeabilized fibres from small biopsies of
1638 muscle, and isolated mitochondria. *Methods Mol Biol* 1782 (Palmeira CM, Moreno AJ, eds): Mitochondrial
1639 Bioenergetics, 978-1-4939-7830-4.
- 1640 Doskey CM, van 't Erve TJ, Wagner BA, Buettner GR (2015) Moles of a substance per cell is a highly informative
1641 dosing metric in cell culture. *PLoS One* 10:e0132572.

- 1642 Drahotka Z, Milerová M, Stieglarová A, Houstek J, Ostádal B (2004) Developmental changes of cytochrome *c*
 1643 oxidase and citrate synthase in rat heart homogenate. *Physiol Res* 53:119-22.
- 1644 Duarte FV, Palmeira CM, Rolo AP (2014) The role of microRNAs in mitochondria: small players acting wide.
 1645 *Genes (Basel)* 5:865-86.
- 1646 Ehinger JK, Morota S, Hansson MJ, Paul G, Elmér E (2015) Mitochondrial dysfunction in blood cells from
 1647 amyotrophic lateral sclerosis patients. *J Neurol* 262:1493-503.
- 1648 Ernster L, Schatz G (1981) Mitochondria: a historical review. *J Cell Biol* 91:227s-55s.
- 1649 Estabrook RW (1967) Mitochondrial respiratory control and the polarographic measurement of ADP:O ratios.
 1650 *Methods Enzymol* 10:41-7.
- 1651 Faber C, Zhu ZJ, Castellino S, Wagner DS, Brown RH, Peterson RA, Gates L, Barton J, Bickett M, Hagerty L,
 1652 Kimbrough C, Sola M, Bailey D, Jordan H, Elangbam CS (2014) Cardiolipin profiles as a potential biomarker
 1653 of mitochondrial health in diet-induced obese mice subjected to exercise, diet-restriction and ephedrine
 1654 treatment. *J Appl Toxicol* 34:1122-9.
- 1655 Feagin JE, Harrell MI, Lee JC, Coe KJ, Sands BH, Cannone JJ, Tami G, Schnare MN, Gutell RR (2012) The
 1656 fragmented mitochondrial ribosomal RNAs of *Plasmodium falciparum*. *PLoS One* 7:e38320.
- 1657 Fell D (1997) Understanding the control of metabolism. Portland Press.
- 1658 Forstner H, Gnaiger E (1983) Calculation of equilibrium oxygen concentration. In: *Polarographic Oxygen Sensors.*
 1659 *Aquatic and Physiological Applications.* Gnaiger E, Forstner H (eds), Springer, Berlin, Heidelberg, New
 1660 York:321-33.
- 1661 Garlid KD, Beavis AD, Ratkje SK (1989) On the nature of ion leaks in energy-transducing membranes. *Biochim*
 1662 *Biophys Acta* 976:109-20.
- 1663 Garlid KD, Semrad C, Zinchenko V. Does redox slip contribute significantly to mitochondrial respiration? In:
 1664 Schuster S, Rigoulet M, Ouhabi R, Mazat J-P, eds (1993) *Modern trends in biothermokinetics.* Plenum Press,
 1665 New York, London:287-93.
- 1666 Gerö D, Szabo C (2016) Glucocorticoids suppress mitochondrial oxidant production via upregulation of
 1667 uncoupling protein 2 in hyperglycemic endothelial cells. *PLoS One* 11:e0154813.
- 1668 Gnaiger E. Efficiency and power strategies under hypoxia. Is low efficiency at high glycolytic ATP production a
 1669 paradox? In: *Surviving Hypoxia: Mechanisms of Control and Adaptation.* Hochachka PW, Lutz PL, Sick T,
 1670 Rosenthal M, Van den Thillart G, eds (1993a) CRC Press, Boca Raton, Ann Arbor, London, Tokyo:77-109.
- 1671 Gnaiger E (1993b) Nonequilibrium thermodynamics of energy transformations. *Pure Appl Chem* 65:1983-2002.
- 1672 Gnaiger E (2001) Bioenergetics at low oxygen: dependence of respiration and phosphorylation on oxygen and
 1673 adenosine diphosphate supply. *Respir Physiol* 128:277-97.
- 1674 Gnaiger E (2009) Capacity of oxidative phosphorylation in human skeletal muscle. *New perspectives of*
 1675 *mitochondrial physiology.* *Int J Biochem Cell Biol* 41:1837-45.
- 1676 Gnaiger E (2014) *Mitochondrial pathways and respiratory control. An introduction to OXPHOS analysis.* 4th ed.
 1677 *Mitochondr Physiol Network* 19.12. Oroboros MiPNet Publications, Innsbruck:80 pp.
- 1678 Gnaiger E, Méndez G, Hand SC (2000) High phosphorylation efficiency and depression of uncoupled respiration
 1679 in mitochondria under hypoxia. *Proc Natl Acad Sci USA* 97:11080-5.
- 1680 Greggio C, Jha P, Kulkarni SS, Lagarrigue S, Broskey NT, Boutant M, Wang X, Conde Alonso S, Ofori E, Auwerx
 1681 J, Cantó C, Amati F (2017) Enhanced respiratory chain supercomplex formation in response to exercise in
 1682 human skeletal muscle. *Cell Metab* 25:301-11.
- 1683 Hinkle PC (2005) P/O ratios of mitochondrial oxidative phosphorylation. *Biochim Biophys Acta* 1706:1-11.
- 1684 Hofstadter DR (1979) Gödel, Escher, Bach: An eternal golden braid. A metaphorical fugue on minds and machines
 1685 in the spirit of Lewis Carroll. Harvester Press:499 pp.
- 1686 Illaste A, Laasmaa M, Peterson P, Vendelin M (2012) Analysis of molecular movement reveals latticelike
 1687 obstructions to diffusion in heart muscle cells. *Biophys J* 102:739-48.
- 1688 Jasienski M, Bazzaz FA (1999) The fallacy of ratios and the testability of models in biology. *Oikos* 84:321-26.
- 1689 Jepihina N, Beraud N, Sepp M, Birkedal R, Vendelin M (2011) Permeabilized rat cardiomyocyte response
 1690 demonstrates intracellular origin of diffusion obstacles. *Biophys J* 101:2112-21.
- 1691 Jezek P, Holendova B, Garlid KD, Jaburek M (2018) Mitochondrial uncoupling proteins: subtle regulators of
 1692 cellular redox signaling. *Antioxid Redox Signal* 29:667-714.
- 1693 Karnkowska A, Vacek V, Zubáčová Z, Treitl SC, Petrželková R, Eme L, Novák L, Žárský V, Barlow LD, Herman
 1694 EK, Soukal P, Hroudová M, Doležal P, Stairs CW, Roger AJ, Eliáš M, Dacks JB, Vlček Č, Hampl V (2016) A
 1695 eukaryote without a mitochondrial organelle. *Curr Biol* 26:1274-84.
- 1696 Kenwood BM, Weaver JL, Bajwa A, Poon IK, Byrne FL, Murrow BA, Calderone JA, Huang L, Divakaruni AS,
 1697 Tomsig JL, Okabe K, Lo RH, Cameron Coleman G, Columbus L, Yan Z, Saucerman JJ, Smith JS, Holmes
 1698 JW, Lynch KR, Ravichandran KS, Uchiyama S, Santos WL, Rogers GW, Okusa MD, Bayliss DA, Hoehn KL
 1699 (2013) Identification of a novel mitochondrial uncoupler that does not depolarize the plasma membrane. *Mol*
 1700 *Metab* 3:114-23.
- 1701 Klepinin A, Ounpuu L, Guzun R, Chekulayev V, Timohhina N, Tepp K, Shevchuk I, Schlattner U, Kaambre T
 1702 (2016) Simple oxygraphic analysis for the presence of adenylate kinase 1 and 2 in normal and tumor cells. *J*
 1703 *Bioenerg Biomembr* 48:531-48.

- 1704 Koit A, Shevchuk I, Ounpuu L, Klepinin A, Chekulayev V, Timohhina N, Tepp K, Puurand M, Truu L, Heck K,
 1705 Valvere V, Guzun R, Kaambre T (2017) Mitochondrial respiration in human colorectal and breast cancer
 1706 clinical material is regulated differently. *Oxid Med Cell Longev* 1372640.
- 1707 Komlódi T, Tretter L (2017) Methylene blue stimulates substrate-level phosphorylation catalysed by succinyl-
 1708 CoA ligase in the citric acid cycle. *Neuropharmacology* 123:287-98.
- 1709 Korn E (1969) Cell membranes: structure and synthesis. *Annu Rev Biochem* 38:263–88.
- 1710 Lai N, M Kummitha C, Rosca MG, Fujioka H, Tandler B, Hoppel CL (2018) Isolation of mitochondrial
 1711 subpopulations from skeletal muscle: optimizing recovery and preserving integrity. *Acta Physiol*
 1712 (Oxf):e13182. doi: 10.1111/apha.13182.
- 1713 Lane N (2005) Power, sex, suicide: mitochondria and the meaning of life. Oxford University Press:354 pp.
- 1714 Larsen S, Nielsen J, Neigaard Nielsen C, Nielsen LB, Wibrand F, Stride N, Schroder HD, Boushel RC, Helge JW,
 1715 Dela F, Hey-Mogensen M (2012) Biomarkers of mitochondrial content in skeletal muscle of healthy young
 1716 human subjects. *J Physiol* 590:3349-60.
- 1717 Lee C, Zeng J, Drew BG, Sallam T, Martin-Montalvo A, Wan J, Kim SJ, Mehta H, Hevener AL, de Cabo R,
 1718 Cohen P (2015) The mitochondrial-derived peptide MOTS-c promotes metabolic homeostasis and reduces
 1719 obesity and insulin resistance. *Cell Metab* 21:443-54.
- 1720 Lee SR, Kim HK, Song IS, Youm J, Dizon LA, Jeong SH, Ko TH, Heo HJ, Ko KS, Rhee BD, Kim N, Han J
 1721 (2013) Glucocorticoids and their receptors: insights into specific roles in mitochondria. *Prog Biophys Mol Biol*
 1722 112:44-54.
- 1723 Leek BT, Mudaliar SR, Henry R, Mathieu-Costello O, Richardson RS (2001) Effect of acute exercise on citrate
 1724 synthase activity in untrained and trained human skeletal muscle. *Am J Physiol Regul Integr Comp Physiol*
 1725 280:R441-7.
- 1726 Lemasters JJ, Nieminen AL, Qian T, Trost LC, Elmore SP, Nishimura Y, Crowe RA, Cascio WE, Bradham CA,
 1727 Brenner DA, Herman B (1998) The mitochondrial permeability transition in cell death: a common mechanism
 1728 in necrosis, apoptosis and autophagy. *Biochim Biophys Acta* 1366:177-96.
- 1729 Lemieux H, Blier PU, Gnaiger E (2017) Remodeling pathway control of mitochondrial respiratory capacity by
 1730 temperature in mouse heart: electron flow through the Q-junction in permeabilized fibers. *Sci Rep* 7:2840.
- 1731 Lenaz G, Tioli G, Falasca AI, Genova ML (2017) Respiratory supercomplexes in mitochondria. In: Mechanisms
 1732 of primary energy transduction in biology. M Wikstrom (ed) Royal Society of Chemistry Publishing, London,
 1733 UK:296-337.
- 1734 Liu S, Roellig DM, Guo Y, Li N, Frace MA, Tang K, Zhang L, Feng Y, Xiao L (2016) Evolution of mitosome
 1735 metabolism and invasion-related proteins in *Cryptosporidium*. *BMC Genomics* 17:1006.
- 1736 Luo S, Valencia CA, Zhang J, Lee NC, Slone J, Gui B, Wang X, Li Z, Dell S, Brown J, Chen SM, Chien YH,
 1737 Hwu WL, Fan PC, Wong LJ, Atwal PS, Huang T (2018) Biparental inheritance of mitochondrial DNA in
 1738 humans. *Proc Natl Acad Sci U S A* doi: 10.1073/pnas.1810946115.
- 1739 Margulis L (1970) Origin of eukaryotic cells. New Haven: Yale University Press.
- 1740 McDonald AE, Vanlerbergh GC, Staples JF (2009) Alternative oxidase in animals: unique characteristics and
 1741 taxonomic distribution. *J Exp Biol* 212:2627-34.
- 1742 Menshikova EV, Ritov VB, Fairfull L, Ferrell RE, Kelley DE, Goodpaster BH (2006) Effects of exercise on
 1743 mitochondrial content and function in aging human skeletal muscle. *J Gerontol A Biol Sci Med Sci* 61:534-40.
- 1744 Menshikova EV, Ritov VB, Ferrell RE, Azuma K, Goodpaster BH, Kelley DE (2007) Characteristics of skeletal
 1745 muscle mitochondrial biogenesis induced by moderate-intensity exercise and weight loss in obesity. *J Appl*
 1746 *Physiol* (1985) 103:21-7.
- 1747 Menshikova EV, Ritov VB, Toledo FG, Ferrell RE, Goodpaster BH, Kelley DE (2005) Effects of weight loss and
 1748 physical activity on skeletal muscle mitochondrial function in obesity. *Am J Physiol Endocrinol Metab*
 1749 288:E818-25.
- 1750 Miller GA (1991) The science of words. Scientific American Library New York:276 pp.
- 1751 Mitchell P (1961) Coupling of phosphorylation to electron and hydrogen transfer by a chemi-osmotic type of
 1752 mechanism. *Nature* 191:144-8.
- 1753 Mitchell P (2011) Chemiosmotic coupling in oxidative and photosynthetic phosphorylation. *Biochim Biophys*
 1754 *Acta Bioenergetics* 1807:1507-38.
- 1755 Mogensen M, Sahlin K, Fernström M, Glintborg D, Vind BF, Beck-Nielsen H, Højlund K (2007) Mitochondrial
 1756 respiration is decreased in skeletal muscle of patients with type 2 diabetes. *Diabetes* 56:1592-9.
- 1757 Mohr PJ, Phillips WD (2015) Dimensionless units in the SI. *Metrologia* 52:40-7.
- 1758 Moreno M, Giacco A, Di Munno C, Goglia F (2017) Direct and rapid effects of 3,5-diiodo-L-thyronine (T2). *Mol*
 1759 *Cell Endocrinol* 7207:30092-8.
- 1760 Morrow RM, Picard M, Derbeneva O, Leipzig J, McManus MJ, Gouspillou G, Barbat-Artigas S, Dos Santos C,
 1761 Hepple RT, Murdock DG, Wallace DC (2017) Mitochondrial energy deficiency leads to hyperproliferation of
 1762 skeletal muscle mitochondria and enhanced insulin sensitivity. *Proc Natl Acad Sci U S A* 114:2705-10.
- 1763 Murley A, Nunnari J (2016) The emerging network of mitochondria-organelle contacts. *Mol Cell* 61:648-53.

- 1764 National Academies of Sciences, Engineering, and Medicine (2018) International coordination for science data
 1765 infrastructure: Proceedings of a workshop—in brief. Washington, DC: The National Academies Press. doi:
 1766 <https://doi.org/10.17226/25015>.
- 1767 Oemer G, Lackner L, Muigg K, Krumschnabel G, Watschinger K, Sailer S, Lindner H, Gnaiger E, Wortmann SB,
 1768 Werner ER, Zschocke J, Keller MA (2018) The molecular structural diversity of mitochondrial cardiolipins.
 1769 Proc Nat Acad Sci U S A 115:4158-63.
- 1770 Palmfeldt J, Bross P (2017) Proteomics of human mitochondria. Mitochondrion 33:2-14.
- 1771 Paradies G, Paradies V, De Benedictis V, Ruggiero FM, Petrosillo G (2014) Functional role of cardiolipin in
 1772 mitochondrial bioenergetics. Biochim Biophys Acta 1837:408-17.
- 1773 Pesta D, Gnaiger E (2012) High-Resolution Respirometry. OXPHOS protocols for human cells and permeabilized
 1774 fibres from small biopsies of human muscle. Methods Mol Biol 810:25-58.
- 1775 Pesta D, Hoppel F, Macek C, Messner H, Faulhaber M, Kobel C, Parson W, Burtscher M, Schocke M, Gnaiger E
 1776 (2011) Similar qualitative and quantitative changes of mitochondrial respiration following strength and
 1777 endurance training in normoxia and hypoxia in sedentary humans. Am J Physiol Regul Integr Comp Physiol
 1778 301:R1078-87.
- 1779 Price TM, Dai Q (2015) The role of a mitochondrial progesterone receptor (PR-M) in progesterone action. Semin
 1780 Reprod Med 33:185-94.
- 1781 Puchowicz MA, Varnes ME, Cohen BH, Friedman NR, Kerr DS, Hoppel CL (2004) Oxidative phosphorylation
 1782 analysis: assessing the integrated functional activity of human skeletal muscle mitochondria – case studies.
 1783 Mitochondrion 4:377-85. Puntschart A, Claassen H, Jostarndt K, Hoppeler H, Billeter R (1995) mRNAs of
 1784 enzymes involved in energy metabolism and mtDNA are increased in endurance-trained athletes. Am J Physiol
 1785 269:C619-25.
- 1786 Quiros PM, Mottis A, Auwerx J (2016) Mitonuclear communication in homeostasis and stress. Nat Rev Mol Cell
 1787 Biol 17:213-26.
- 1788 Rackham O, Mercer TR, Filipovska A (2012) The human mitochondrial transcriptome and the RNA-binding
 1789 proteins that regulate its expression. WIREs RNA 3:675-95.
- 1790 Rackham O, Shearwood AM, Mercer TR, Davies SM, Mattick JS, Filipovska A (2011) Long noncoding RNAs
 1791 are generated from the mitochondrial genome and regulated by nuclear-encoded proteins. RNA 17:2085-93.
- 1792 Reichmann H, Hoppeler H, Mathieu-Costello O, von Bergen F, Pette D (1985) Biochemical and ultrastructural
 1793 changes of skeletal muscle mitochondria after chronic electrical stimulation in rabbits. Pflugers Arch 404:1-9.
- 1794 Renner K, Amberger A, Konwalinka G, Gnaiger E (2003) Changes of mitochondrial respiration, mitochondrial
 1795 content and cell size after induction of apoptosis in leukemia cells. Biochim Biophys Acta 1642:115-23.
- 1796 Rice DW, Alverson AJ, Richardson AO, Young GJ, Sanchez-Puerta MV, Munzinger J, Barry K, Boore JL, Zhang
 1797 Y, dePamphilis CW, Knox EB, Palmer JD (2016) Horizontal transfer of entire genomes via mitochondrial
 1798 fusion in the angiosperm *Amborella*. Science 342:1468-73.
- 1799 Rich P (2003) Chemiosmotic coupling: The cost of living. Nature 421:583.
- 1800 Rich PR (2013) Chemiosmotic theory. Encyclopedia Biol Chem 1:467-72.
- 1801 Roger JA, Munoz-Gomes SA, Kamikawa R (2017) The origin and diversification of mitochondria. Curr Biol
 1802 27:R1177-92.
- 1803 Rostovtseva TK, Sheldon KL, Hassanzadeh E, Monge C, Saks V, Bezrukov SM, Sackett DL (2008) Tubulin
 1804 binding blocks mitochondrial voltage-dependent anion channel and regulates respiration. Proc Natl Acad Sci
 1805 USA 105:18746-51.
- 1806 Rustin P, Parfait B, Chretien D, Bourgeron T, Djouadi F, Bastin J, Rötig A, Munnich A (1996) Fluxes of
 1807 nicotinamide adenine dinucleotides through mitochondrial membranes in human cultured cells. J Biol Chem
 1808 271:14785-90.
- 1809 Saks VA, Veksler VI, Kuznetsov AV, Kay L, Sikk P, Tiivel T, Tranqui L, Olivares J, Winkler K, Wiedemann F,
 1810 Kunz WS (1998) Permeabilised cell and skinned fiber techniques in studies of mitochondrial function in vivo.
 1811 Mol Cell Biochem 184:81-100.
- 1812 Salabei JK, Gibb AA, Hill BG (2014) Comprehensive measurement of respiratory activity in permeabilized cells
 1813 using extracellular flux analysis. Nat Protoc 9:421-38.
- 1814 Sazanov LA (2015) A giant molecular proton pump: structure and mechanism of respiratory complex I. Nat Rev
 1815 Mol Cell Biol 16:375-88.
- 1816 Schneider TD (2006) Claude Shannon: biologist. The founder of information theory used biology to formulate the
 1817 channel capacity. IEEE Eng Med Biol Mag 25:30-3.
- 1818 Schönfeld P, Dymkowska D, Wojtczak L (2009) Acyl-CoA-induced generation of reactive oxygen species in
 1819 mitochondrial preparations is due to the presence of peroxisomes. Free Radic Biol Med 47:503-9.
- 1820 Schultz J, Wiesner RJ (2000) Proliferation of mitochondria in chronically stimulated rabbit skeletal muscle--
 1821 transcription of mitochondrial genes and copy number of mitochondrial DNA. J Bioenerg Biomembr 32:627-
 1822 34.
- 1823 Speijer D (2016) Being right on Q: shaping eukaryotic evolution. Biochem J 473:4103-27.
- 1824 Sugiura A, Mattie S, Prudent J, McBride HM (2017) Newly born peroxisomes are a hybrid of mitochondrial and
 1825 ER-derived pre-peroxisomes. Nature 542:251-4.

- 1826 Simson P, Jepihhina N, Laasmaa M, Peterson P, Birkedal R, Vendelin M (2016) Restricted ADP movement in
1827 cardiomyocytes: Cytosolic diffusion obstacles are complemented with a small number of open mitochondrial
1828 voltage-dependent anion channels. *J Mol Cell Cardiol* 97:197-203.
- 1829 Singh BK, Sinha RA, Tripathi M, Mendoza A, Ohba K, Sy JAC, Xie SY, Zhou J, Ho JP, Chang CY, Wu Y,
1830 Giguère V, Bay BH, Vanacker JM, Ghosh S, Gauthier K, Hollenberg AN, McDonnell DP, Yen PM (2018)
1831 Thyroid hormone receptor and ERR α coordinately regulate mitochondrial fission, mitophagy, biogenesis, and
1832 function. *Sci Signal* 11(536) DOI: 10.1126/scisignal.aam5855.
- 1833 Stucki JW, Ineichen EA (1974) Energy dissipation by calcium recycling and the efficiency of calcium transport in
1834 rat-liver mitochondria. *Eur J Biochem* 48:365-75.
- 1835 Tonkonogi M, Harris B, Sahlin K (1997) Increased activity of citrate synthase in human skeletal muscle after a
1836 single bout of prolonged exercise. *Acta Physiol Scand* 161:435-6.
- 1837 Torralba D, Baixauli F, Sánchez-Madrid F (2016) Mitochondria know no boundaries: mechanisms and functions
1838 of intercellular mitochondrial transfer. *Front Cell Dev Biol* 4:107. eCollection 2016.
- 1839 Vamecq J, Schepers L, Parmentier G, Mannaerts GP (1987) Inhibition of peroxisomal fatty acyl-CoA oxidase by
1840 antimycin A. *Biochem J* 248:603-7.
- 1841 Waczulikova I, Habodaszova D, Cagalinec M, Ferko M, Ulicna O, Mateasik A, Sikurova L, Ziegelhöffer A (2007)
1842 Mitochondrial membrane fluidity, potential, and calcium transients in the myocardium from acute diabetic rats.
1843 *Can J Physiol Pharmacol* 85:372-81.
- 1844 Wagner BA, Venkataraman S, Buettner GR (2011) The rate of oxygen utilization by cells. *Free Radic Biol Med*
1845 51:700-712.
- 1846 Wang H, Hiatt WR, Barstow TJ, Brass EP (1999) Relationships between muscle mitochondrial DNA content,
1847 mitochondrial enzyme activity and oxidative capacity in man: alterations with disease. *Eur J Appl Physiol*
1848 *Occup Physiol* 80:22-7.
- 1849 Watt IN, Montgomery MG, Runswick MJ, Leslie AG, Walker JE (2010) Bioenergetic cost of making an adenosine
1850 triphosphate molecule in animal mitochondria. *Proc Natl Acad Sci U S A* 107:16823-7.
- 1851 Weibel ER, Hoppeler H (2005) Exercise-induced maximal metabolic rate scales with muscle aerobic capacity. *J*
1852 *Exp Biol* 208:1635-44.
- 1853 White DJ, Wolff JN, Pierson M, Gemmell NJ (2008) Revealing the hidden complexities of mtDNA inheritance.
1854 *Mol Ecol* 17:4925-42.
- 1855 Wikström M, Hummer G (2012) Stoichiometry of proton translocation by respiratory complex I and its
1856 mechanistic implications. *Proc Natl Acad Sci U S A* 109:4431-6.
- 1857 Williams EG, Wu Y, Jha P, Dubuis S, Blattmann P, Argmann CA, Houten SM, Amariuta T, Wolski W, Zamboni
1858 N, Aebersold R, Auwerx J (2016) Systems proteomics of liver mitochondria function. *Science* 352
1859 (6291):aad0189
- 1860 Willis WT, Jackman MR, Messer JI, Kuzmiak-Glancy S, Glancy B (2016) A simple hydraulic analog model of
1861 oxidative phosphorylation. *Med Sci Sports Exerc* 48:990-1000.
- 1862 Zíková A, Hampl V, Paris Z, Týč J, Lukeš J (2016) Aerobic mitochondria of parasitic protists: diverse genomes
1863 and complex functions. *Mol Biochem Parasitol* 209:46-57.
- 1864
- 1865

1866 **Supplement**

1867

1868 **S1. Manuscript phases and versions - an open-access approach**

1869

1870 This manuscript on ‘Mitochondrial respiratory states and rates’ is a position statement in the frame of COST Action
 1871 CA15203 MitoEAGLE. The global MitoEAGLE network made it possible to collaborate with a large number of
 1872 coauthors to reach consensus on the present manuscript. Nevertheless, we do not consider scientific progress to be
 1873 supported by ‘declaration’ statements (other than on ethical or political issues). Our manuscript aims at providing
 1874 arguments for further debate rather than pushing opinions. We hope to initiate a much broader process of
 1875 discussion and want to raise the awareness of the importance of a consistent terminology for reporting of scientific
 1876 data in the field of bioenergetics, mitochondrial physiology and pathology. Quality of research requires quality of
 1877 communication. Some established researchers in the field may not want to re-consider the use of jargon which has
 1878 become established despite deficiencies of accuracy and meaning. In the long run, superior standards will become
 1879 accepted. We hope to contribute to this evolutionary process, with an emphasis on harmonization rather than
 1880 standardization.

1881 *Phase 1* The protonmotive force and respiratory control1882 http://www.mitoeagle.org/index.php/The_protonmotive_force_and_respiratory_control

1883 • 2017-04-09 to 2017-09-18 (44 versions) / 2017-09-21 to 2018-02-06 (44 plus 21 versions)

1884 http://www.mitoeagle.org/index.php/MitoEAGLE_preprint_2017-09-21

1885 2017-11-11: Print version (16) for MiP2017/MitoEAGLE conference in Hradec Kralove

1886 *Phase 2* Mitochondrial respiratory states and rates: Building blocks of mitochondrial physiology Part 11887 http://www.mitoeagle.org/index.php/MitoEAGLE_preprint_States_and_rates

1888 • 2018-02-08 – 2019-01-24 (44 plus 52 Versions)

1889 *Phase 3* Journal submission: CELL METABOLISM, aiming at indexing by *The Web of Science* and *PubMed*.

1890

1891 **S2. Joining COST Actions**

1892

1893 • CA15203 MitoEAGLE - http://www.cost.eu/COST_Actions/ca/CA152031894 • CA16225 EU-CARDIOPROTECTION - http://www.cost.eu/COST_Actions/ca/CA162251895 • CA17129 CardioRNA - http://www.cost.eu/COST_Actions/ca/CA17129

1896

COST Action CA15203 MitoEAGLE

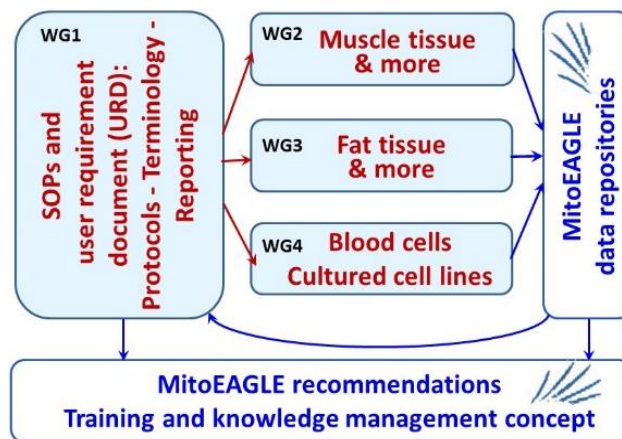
Evolution Age Gender
Lifestyle Environment



Mission of the global MitoEAGLE network

in collaboration with the Mitochondrial Physiology Society, MiPs

- Improve our knowledge on mitochondrial function in health and disease with regard to Evolution, Age, Gender, Lifestyle and Environment
- Interrelate studies across laboratories with the help of a MitoEAGLE data management system
- Provide standardized measures to link mitochondrial and physiological performance to understand the myriad of factors that play a role in mitochondrial physiology



Join the COST Action MitoEAGLE - contribute to the quality management network.



More information:
www.mitoeagle.org

